TOWARDS RABI OSCILLATIONS MEASUREMENTS IN NV CENTERS

DEVELOPMENT OF A QUANTUM CONTROL SETUP FOR NV CENTERS WITH CHARACTERISATION

Thesis

To obtain the degree of Bachelor of Science
at the Delft University of Technology,
to be defended publicly on Tuesday June 24, 2025 at 15:30 PM.

by

Jurre BOTMAN, Seppe DIJKSTRA

Student number:	Jurre Botman	5788641
	Seppe Dijkstra	5803632
Project duration:	April 22, 2025 - June 24, 2025	
Thesis committee:	S. Nur,	TU Delft, supervisor
	Dr. IR. M.A.P. Pertijs,	TU Delft
	Dr. S. Izadkhast,	TU Delft

ABSTRACT

In this work, we aim to characterize the Rabi oscillations of nitrogen-vacancy (NV) centers in diamond by implementing and utilizing a tailored experimental setup, where optical pulses are produced by an acousto-optic modulator (AOM). A central focus of this thesis was to design and construct a custom AOM around a TeO2 crystal. This was a necessity, because the commercial AOM failed during one of the experiments. The work that has been done involved extensive characterization of precise and synchronized timing. High-quality Rabi oscillations could not be measured due to time limitations and the breaking down of the commercial AOM. However, the thesis shows full control over pulse-sequencing, optical microwaves and NV excitation. This work provides a foundation for further spin dynamic experiments of NV centers. During the thesis software for controlled timing has been built, and the designing and integration of custom made electronics has been done, which can provide practical guidance for controlling quantum instrumentation devices. We highlight the engineering challenges in building quantum instrumentation from the ground up.

CONTENTS

1 Introduction **1**

2 Background knowledge **3**
2.1 NV centers . . . 3
2.2 Spin System . . . 4
2.3 Energy level diagram . . . 5
2.4 CW ODMR . . . 6
2.5 Rabi oscillations . . . 6
2.6 Zeeman effect . . . 7
2.7 Measuring Rabi oscillations . . . 9
2.7.1 Time-domain Rabi measurement . . . 9
2.7.2 Optomechanical quantum control . . . 10
2.8 Acousto-optic modulator . . . 11
2.8.1 Basic principle . . . 12
2.8.2 Controlling the AOM . . . 12

3 Requirements **14**

4 Measurement Procedures **15**
4.1 Measurement setup . . . 15
4.2 Controlling the setup . . . 16
4.3 Proposed method . . . 17

5 AOM Design and Testing **20**
5.1 Commercial AOM and driver . . . 20
5.1.1 AOM . . . 20
5.1.2 RF driver . . . 21
5.1.3 Failure . . . 21
5.2 Testing the crystal . . . 23
5.2.1 Piezoelectric effect . . . 23
5.2.2 Impedance of the crystal . . . 24
5.3 Designing the matching circuit . . . 24
5.3.1 L-networks . . . 25
5.3.2 Q factor . . . 26
5.3.3 Resistance Matching . . . 26
5.3.4 Component Values . . . 27
5.3.5 Absorption . . . 28
5.3.6 Simulation . . . 28
5.4 Testing the custom built AOM . . . 29

6 Results **32**
6.1 Testing the measurement setup . . . 32
6.1.1 AWG . . . 32
6.1.2 ODMR . . . 33
6.2 Rabi oscillations . . . 34

7 Discussion **36**

8 Conclusion and outlook **38**
8.1 Rabi oscillations . . . 38
8.2 AOM . . . 38
8.3 Outlook . . . 39

A Overview of code **44**
A.1 ESR Measurement . . . 44
A.2 Rabi Oscillation Measurement . . . 46
A.3 AWG Oscilloscope Graphs . . . 49
A.4 Piezoelectric effect plot . . . 51
A.5 Impedance Matching Simulation . . . 51
A.6 Processing the Rabi oscillations and fitting the data . . . 53
A.7 VNA AOM measurement graph . . . 54

1

INTRODUCTION

Quantum sensing based on nitrogen vacancy (NV) centers in diamond has proven to be a promising field towards the imaging of a magnetic field. Due to the long coherence time of NV centers at room temperature, it has proven to be a leading candidate for quantum sensors [1], [2]. This thesis contributes to a larger project aimed at the development of an on-chip SPAD quantum image sensor based on NV-centers in diamond for high-sensitivity and high-accuracy sensing of bio-samples, see Figure 1.1 [3]. An application in the field of bio-sensing would be, for instance, the submersion of human cells in a solution of magnetic nanoparticles (MNP). These nanoparticles make the submerged cells responsive to magnetism, which allows for the detection of malignant cells. However, to distinguish malignant cells from healthy ones, selective MNPs are used. These nanoparticles can be paired with antibodies that specifically bind to malignant cells. This selective binding makes the malignant cells effectively magnetic, which makes it possible to detect them. [3].

The goal of this thesis specifically is to measure the Rabi oscillations of the NV centers. To be able to perform these measurements, a custom-built acousto-optic modulator (AOM) must be designed. Rabi oscillations can help characterize the diamond sample and improve the setup, as they describe the exact state of the matter interacting with a driving field. Knowing the Rabi frequency allows for precise tuning of the measurement setup, such as the external field, based on characteristics of the NV centers. Moreover, with the measurement of the Rabi oscillations, it is possible to perform single-qubit gate operations and characterize the diamond sample that is used. The ability to perform these single-qubit gate operations leads to advanced measurement protocols, which will be able to remove noise. This can lead to better and more accurate measurements [5].

This report will start with the background knowledge, here all the information that is needed for further reading will be discussed. Moreover, the different methods to measure Rabi oscillations will be discussed. The next chapter will discuss all the requirements, where we have to adhere to. This chapter will be followed up with the measure-

1

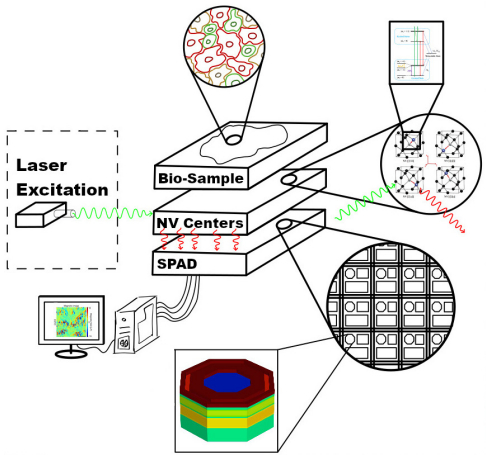

Figure 1.1: General overview of the full system used for magnetic bio-imaging, showing the main components of the systems, the bio-sample, NV centers, laser excitation system, and SPAD sensor [4]

ment procedures, this chapter will provide information about the current measurement setup, the controlling of this setup, and the experiments that will be performed. The chapter AOM design and testing will start with the current situation and why a custom-built AOM is needed. The chapter will finalize with a new design of a custom-built AOM and its testing. Then the results will be discussed. In this chapter, all the results that were obtained with the commercial AOM will be presented. In discussion, all the problems and fixes that occurred during the thesis will be talked over. The thesis will end with a conclusion and outlook of the whole thesis.

2

BACKGROUND KNOWLEDGE

The goal of this thesis is to measure Rabi oscillations. Before talking about Rabi oscillations, it is important to have an understanding of how measurements of NV centers can be done. In short, a green laser will be aimed at the diamond lattice with NV centers in it. NV centers is short for nitrogen-vacancy centers and will later on be explained in more depth. The green laser will then excite electrons to an excited state. These electrons cannot stay there for long and will decay back to the ground state. During this process red light will be emitted. The intensity of this red light can be detected by the Single Photon Avalanche Diode (SPAD). However, it is also possible that the electrons decay via a different path. When decaying via this path, it will emit infrared light instead of red visible light. This means that the total intensity of red light will be lower when it can also decay via this alternative path. When there is an external magnetic field present, the Zeeman effect occurs. The Zeeman effect can also have an effect on the emitted red light. Thus, with the SPAD it will be possible to detect changes in the intensity of the red light. From these measurements you can draw conclusions about the external magnetic field. How this works in detail will be explained in the coming subsections with the theory behind it.

2.1. NV CENTERS

As discussed before, we have a certain material where a green light is being shone on. This material is a diamond structure with NV centers in it. NV centers are point defects where two adjacent carbon atoms are substituted by a nitrogen atom next to a vacancy. The NV center can be electrically neutral (NV^0 center) or can capture an additional free-floating electron from the conduction band, forming a negatively charged (NV^-) center. Multiple properties, such as a long spin coherence time and the ability to be optically initialized and read out, make NV^- centers an ideal physical system for quantum sensing applications. Henceforth, NV^- centers will be called NV centers.

Nitrogen atoms can be inserted in a diamond lattice with ion implantation, or the diamond can be doped during the chemical vapor deposition growth process. Then the

vacancies can be created by means of laser irradiation, ion implantation, or electron irradiation. Lastly, the material is heated above its recrystallization temperature to form the NV centers. [6]

2

2.2. SPIN SYSTEM

First, it is good to have an understanding about spin. Spin is a property of a particle, and represents the intrinsic angular momentum. This angular momentum can imply the particle is spinning, but this is a misconception. Spin will be denoted as follows $|S, m\rangle$, with S, being the total spin and m_s the spin projection. This $|\rangle$, may be unfamiliar, but the only thing it describes is a column vector. For a quantum system this S always has the same value for a specific system. However, this m_s could be different for this specific system. It has different possibilities and the possibilities easily be calculated with Equation . So when we for example have a spin-$\frac{1}{2}$ system we know $S = \frac{1}{2}$ and then $m_s = -\frac{1}{2}, \frac{1}{2}$.

$$m_s \in \{-S, -S+1, ..., S\}, \tag{2.1}$$

An NV^- center has two free electrons. An electron is a spin $\frac{1}{2}$-system, because they are fermions. Because we have two free electrons, there is coupling between them, and they will form a combined spin system. For simplicity, we will refer to this spin system as a qubit. Combining these two spin $\frac{1}{2}$-systems will result in a spin 1-system, this spin is illustrated below. This information has been based on the Griffiths book [7].
Triplet state (s=1):

$$|11\rangle = \uparrow\uparrow \quad |10\rangle = \frac{1}{\sqrt{2}}(\uparrow\downarrow + \downarrow\uparrow) \quad |1\ -1\rangle = \downarrow\downarrow \tag{2.2}$$

Singlet state (s=0):

$$|00\rangle = \frac{1}{\sqrt{2}}(\uparrow\downarrow - \downarrow\uparrow) \tag{2.3}$$

To have a better understanding of spin states and what they represent, we can have a look at Figure 2.1. The Bloch Sphere provides an intuitive way to visualize these spin states. The top will represent the zero spin, and the bottom the ±1 spin. A qubit can, in theory, have all the spin states on this Bloch sphere. Only when measured will it collapse in one defined state. So when looking at the picture again, it can be seen that this $|\Psi\rangle$ will represent our qubit. When measuring this, there will be a higher change of measuring $|0\rangle$, than $|1\rangle$. This means that the qubit is in superposition of $|1\rangle$ and $|0\rangle$, so the spin state is probabilistic. This property will be used to measure the Rabi oscillations, and it will be explained in greater detail later on.

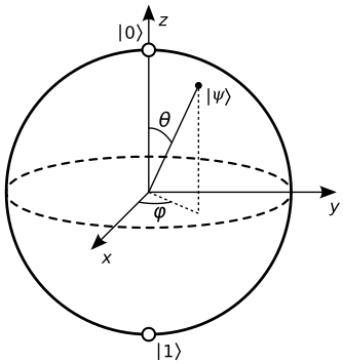

Figure 2.1: Bloch Sphere, extracted from [8]

2.3. ENERGY LEVEL DIAGRAM

In Figure 2.2, the energy diagram of the NV center can be seen. The ground state and the excited state are spin triplets, while the metastable state is a spin singlet. The ground state is the lowest possible energy level that the atom can occupy. These states are split into multiple levels due to the differences in energy of the spin states. $m_s = \pm 1$ has a higher energy level than $m_s = 0$, where $m_s = +1$ has an even slightly higher energy than $m_s = -1$. The splitting between $m_s = 0$ and $m_s = \pm 1$ is called the zero-field splitting, as it is present even without any external fields, and it corresponds to a Bohr frequency of 2.87 GHz.

Upon excitation with a green laser, electrons can transfer the gap between the ground state and the excited state. When they fall back, they emit a red photon. Both of these processes are spin-conserving. In addition to the radiative channels, electrons in the excited level with spin ±1 may decay non-radiatively through the shelving state, ending up primarily in the ground state. This allows for the spin state of the system to be reset by a green laser. [9]

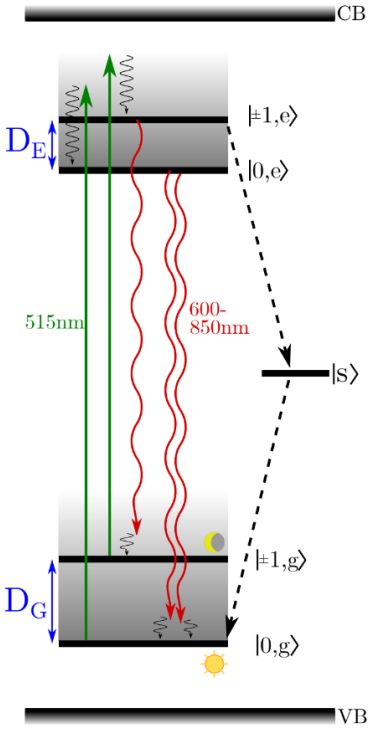

Figure 2.2: Simplified energy diagram of the NV center

2.4. CW ODMR

Due to the non-radiative decay path through the shelf state, there is less fluorescence when the system is in $|\pm1\rangle$. By measuring the fluorescence, the spin state can be determined. An optically detected magnetic resonance (ODMR) spectrum is created by applying a continuous wave (CW) external microwave field and sweeping the frequency while monitoring the fluorescence. When the microwave frequency is the same as the energy gap between the ms=0 and ms=pm1 spin states, the system will resonate with the microwaves and the spins will change. This can be seen as a dip in the fluorescence. In Figure 2.3, the ODMR spectrum can be seen. This is the situation when the NV centers are at room temperature and the qubits are being excited with a 532 nm laser. This will result in less red light and more infrared light that is being emitted at around 2.87 GHz, [10].

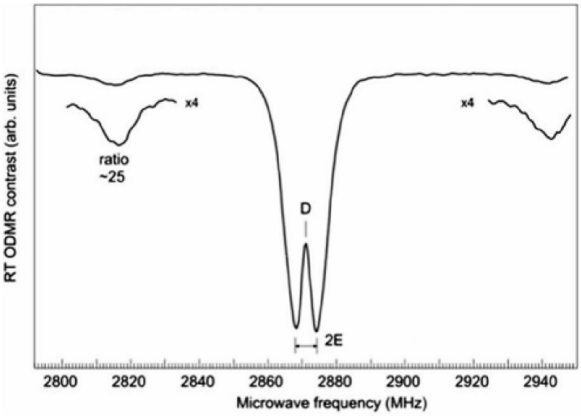

Figure 2.3: ODMR spectrum when the qubit is excited with a 532nm laser. Adapted from [11]

2.5. RABI OSCILLATIONS

Rabi oscillations describe the exact state of a matter interacting with a driving field. A Rabi cycle is the cyclic behavior of a two-level quantum system in the presence of an oscillatory near-resonant driving field. In the NV center, this is the oscillation of the electrons between their spin states. As said before, this will only occur when a microwave field is applied with the frequency of the dip in Figure 2.3. The oscillations of spin states can be between $|0,g\rangle$ and $|\pm1,g\rangle$, but also between $|0,e\rangle$ and $|\pm1,e\rangle$. These states can be found in Figure 2.2. The frequencies with which these spin state oscillations take place are called Rabi frequencies. The Rabi frequency is proportional to the oscillatory driving field applied and to the strength of the electron coupling. To give a more clear description of how these spin transitions work, we can have a look at Figure 2.4. In this figure you can see that initially the spin state is equal to $|0\rangle$. But when an MW pulse is applied, this state will land somewhere in between the $|0\rangle$ and $|1\rangle$ spin states. By applying a longer MW pulse, this spin state will go even further, and we will have another probability. And this phenomenon is called Rabi oscillations.

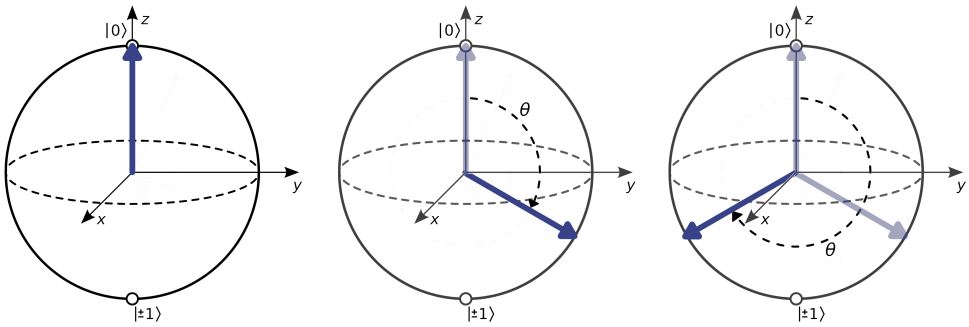

Figure 2.4: The Bloch sphere of the NV center qubit after applying different duration of a RF wave

Knowing the Rabi frequency allows for precisely tuning the measurement setup, such as the external field, as it describes the state of matter of the NV center. The oscillation frequency gets larger and the amplitude smaller with increasing detuning of the driving field. [12]

2.6. ZEEMAN EFFECT

The Zeeman effect is a phenomenon that occurs when the system is present in a magnetic field. This magnetic field influences the total Hamiltonian [1] of the system, thus we have a perturbation. This perturbation is described in Equation [2]2.4 [10].

$$H_{int}/h = \frac{g_e \mu_B}{h}(B^\dagger \hat{S}) = \overline{\gamma}_{NV} B^\dagger \hat{S} \tag{2.4}$$

This μ_B is the Bohr magneton, which is described as $\mu_B = \frac{e\hbar}{2m}$. The symbol $\overline{\gamma}_{NV}$ is the NV gyromagnetic ratio and is a constant value equal to $28 MHz/mT$. This equation shows that when an external magnetic field is applied, the spin states $|+1\rangle$ and $|-1\rangle$, will split.

[1] Hamiltonian in quantum mechanics is the total energy of the system, most times described as the addition of all the kinetic and potential energies.

[2] In the equation this $\hat{S}$ means a spin operator. So for example it will be acting on $|S, m_s\rangle$, you will get $\hat{S}|S, m_s\rangle = \hbar m_s$

The qubit that exist in the NV centers can have spin states of $m_s = -1, 0, 1$. This means that different spin states have different energies. To visualize this a new energy level diagram will be needed, this diagram can be found in Figure 2.5. In this figure it can be seen that the differences in energy between the states $m_s = -1$ and 1 is equal to $2g\mu_B B$. g is the Landé factor, which accounts for the effect on both m_s and m_l in the presence of a magnetic field. This difference in energy is what was expected when looking at Equation 2.4, due to spin-orbit coupling, this Landé factor is needed.

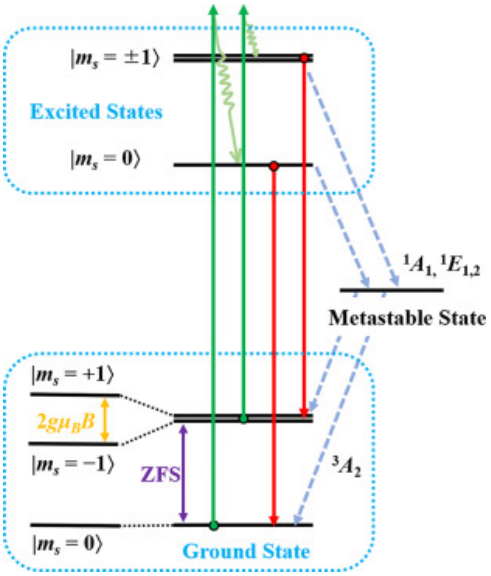

Figure 2.5: Energy-level diagram with the Zeeman effect, extracted from [13]

As explained before, when the ODMR spectrum is measured, a resonance peak at $2.87 GHz$ can be seen. However, when this same sweep over a frequency range is done again, but with an external magnetic field, you will see something different. And this is due to the Zeeman effect explained before. First, the plot can be seen in Figure 2.6.

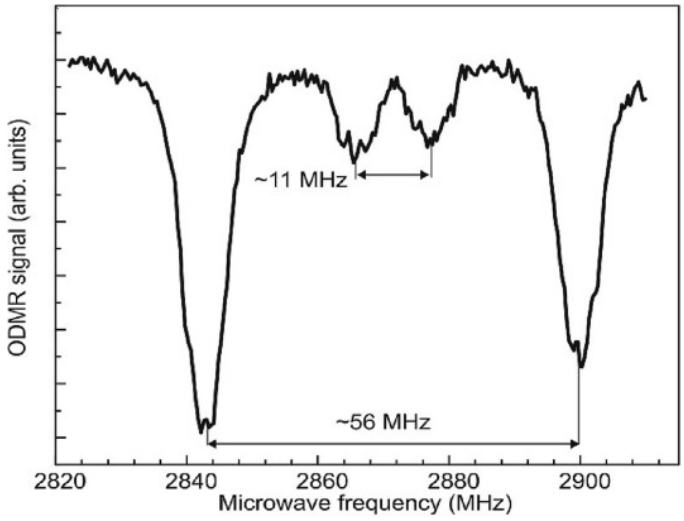

Figure 2.6: The ODMR spectrum when an external magnetic field is present. Measured when the qubits are being excited with a laser of 532 nm and at room temperature

Comparing this figure with Figure 2.3 it can be seen that now 2 peaks are present. This is because the energies of the $|\pm 1\rangle$ are not equal to each other. The difference in energy between the two was discussed before and was equal to $2g\mu_B B$. It is known that to get the frequency from the Hamiltonian, we can easily divide by Planck's constant. Thus the frequency difference of these two peaks can be described as in Equation 2.5, as has been discussed in [10]. This $\overline{\gamma}_{NV} \approx 28\ MHz/mT$ is the reduced NV gyromagnetic ratio and has a value of $\approx 28\ MHz/mT$.

$$\Delta\nu = \frac{2g\mu_B}{h} B = 2\overline{\gamma}_{NV} \cdot B \tag{2.5}$$

Thus, with Figure 2.6 we can precisely determine the magnetic field because we have the frequency difference between the two peaks.

2.7. MEASURING RABI OSCILLATIONS

To determine the Rabi oscillations, we will look at different available methods. The determination of Rabi oscillations is something that has been done a lot over the years and will give us more insight into the NV-centers that will be used. Measuring Rabi oscillations can tell a lot of information about the quality of the setup and is important for gate operations.

2.7.1. TIME-DOMAIN RABI MEASUREMENT

Time-domain Rabi measurement is a simplistic, widely used method [12], [14]–[16]. The timing for these measurements depends on what kind of NV centers are used and their purity.

The experiment will start by emitting a laser of 532 nm on the crystal structure. This will polarize the system in the $|0\rangle$ spin state. Then there must be a small delay, called padding. This is necessary for the depletion of the shelf state. As explained in Section 2.5, applying an RF wave has the possibility of moving the qubit to the $|\pm 1\rangle$ spin state. This RF wave will have the duration τ. After this RF wave, we want to measure the amount of qubits that have been excited to the $|\pm 1\rangle$ spin state. This can be done by measuring the photoluminescence. Measuring this photoluminescence can be done by again emitting the green laser on the diamond and turning on the single photon avalanche detector (SPAD).
Notice that we have stated that the duration of the RF wave will be τ. This is because we want to use different lengths of this RF pulse since the timing is important for the probability of exciting to the $|\pm 1\rangle$ spin state. So to get a clear Rabi frequency, we need to sweep over different lengths. Since everything is a probability and can change for every experiment, we want to repeat this whole sweep many times. This will reduce outliers. A clear schematic of this experiment can be found in Figure 2.7. Notice that there is also a readout of the SPAD before the RF pulse. If everything works accordingly, this will measure the noise. This noise will be background photons that must not be accounted for after the RF wave.

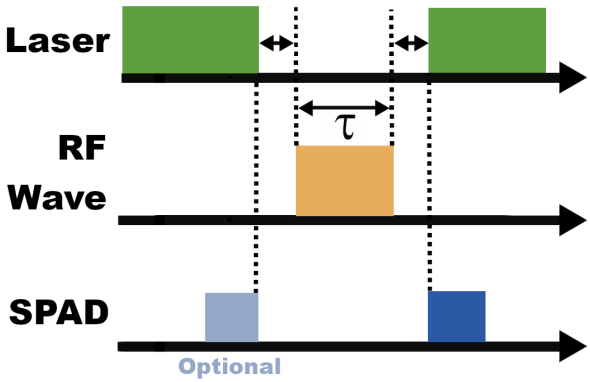

Figure 2.7: Schematic that describes the Time-domain Rabi measurement

2.7.2. OPTOMECHANICAL QUANTUM CONTROL

So far we have discussed a method that uses RF waves. But RF waves could be hard to control if used in a scalable application. So to prevent this, we need a method that will not use an RF field. A method that does this is the optomechanical quantum control. With this optomechanical control, there will be an interaction between the photons and phonons. The following papers [17], [18] discuss this method. In the papers, the mechanical control will be done with the help of a standing acoustic wave, SAW for short.

A SAW can be generated by applying an RF signal to an inter digital transducer, (IDT) on a piezoelectric material. Such a configuration can be found in Figure 2.8b. A SAW can couple the spin state of the NV center to a mechanical mode. The frequency of the SAW will be denoted as ω_m and has been estimated in [17] as $900MHz$.

To explain the experiment to determine the Rabi oscillations, we need to know more about the optomechanical control. In an energy level spectrum, there is a Zero-Phonon Line (ZPL). This is the energy needed to have a transition to the excited state without the need for vibrations or phonons. The ZPL for NV centers is at a wavelength of $\lambda = 637nm$. So when we have a laser that is slightly detuned from this ZPL, there can still be transitions, but only if vibrations or phonons are present. That is why the SAW field will be important for this experiment. In Figure 2.8c, you can see the red and blue sideband transitions. The red sideband transition needs to absorb a phonon to have enough energy, and the blue sideband needs to emit a phonon.
The experiment to measure the Rabi oscillations works similarly to the time-domain Rabi oscillations experiment. However, there are some differences. This experiment still uses the green light to initialize all the spin states. But now there is an extra laser present, which is slightly detuned. You can use both sideband transitions, but for this experiment, the red sideband transition is used. As explained before, to excite a qubit with the red sideband transitions, a phonon must be absorbed with a frequency of $w_m = 900MHz$. To create Rabi oscillations, we must vary the timing of when the SAW field is on, which will be denoted as τ in Figure 2.9. During the SAW field, the the photoluminescence must

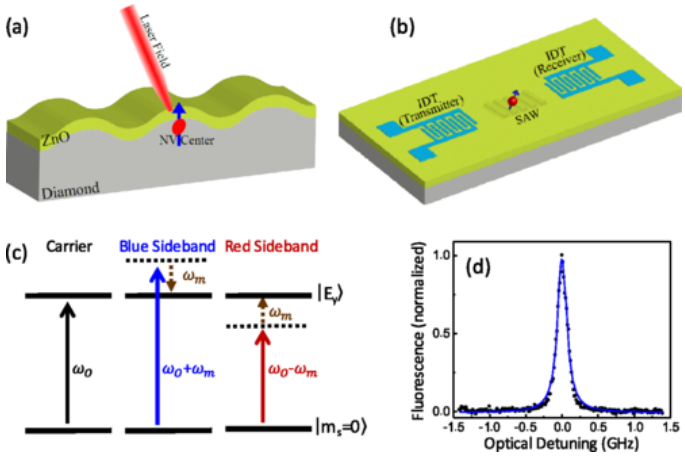

Figure 2.8: a) Shows the NV-center in the ZnO substrate, with a red laser being emitted on the NV-center. b) Shows the substrate with the transmitting and receiving IDT. These IDTs are made with lithography. c) Here the sideband and the ZPL transmission can be seen. Both sidebands are off by a small factor ω_m. d) This plot shows the optical detuning for the ZPL. It can be seen that when the frequency is detuned, no fluorescence is measured. Extracted from [17]

be detected. The initializing laser must be done once, then all the measurements can be done.

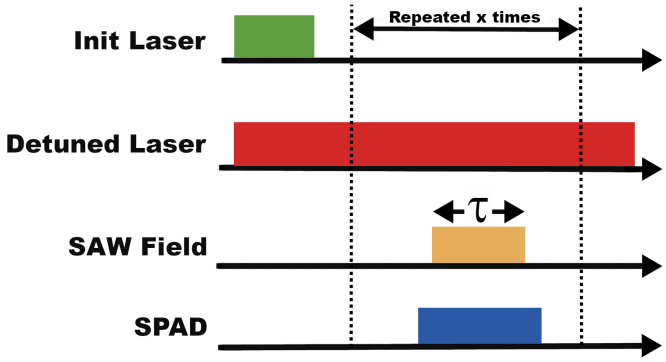

Figure 2.9: Schematic that describes the optomechanical Rabi measurement

2.8. ACOUSTO-OPTIC MODULATOR

In the previous section it became clear that we need to control a light pulse. This light pulse needs to be able to turn on and off in a short period of time, in the μ seconds. In the industry one device is widely used, this device is an acousto-optic modulator, or AOM for short. An AOM allows the direction of a laser beam to be modulated. This modulation is happening due to a laser beam Bragg diffracting while it is propagating through a crystal. This diffraction can be controlled by varying the acoustics waves that will travel through

the crystal. There are two basic AOMs, namely the Raman-Nath type and Bragg-type modulators. For this report we will only talk about the Bragg-type modulators, since those are the ones that are used for these kinds of applications.

2

2.8.1. BASIC PRINCIPLE

The AOM works based on the Bragg condition, which describes the constructive interference of waves. In the case of an AOM, we have the light that scatters off a moving diffraction grating. A diffraction grating in this case is a periodic modulation of the refractive index. The moving diffraction grating is caused by mechanical strain that is present in the crystal, also called the photoelastic effect. This mechanical strain is produced by the acoustic waves that are traveling through the crystal. In Formula 2.6 [19] the changes in the refractive index, (Δn) can be found in relation to the acoustic power P_a. This formula shows us that the refractive index changes on the amount of refractive index.

$$\Delta n = \sqrt{\frac{n^6 p^2 10^7 P_a}{2Q v_a^3 A}} \tag{2.6}$$

The Bragg condition for constructive interference of the scattered light can be approximated as in Formula 2.7 [20]. Where λ_L is the wavelength of the emitted light, which is $532nm$. The Δ is the distance between the planes of the diffraction grating. These distances are equal to the wavelength of the acoustic wave. Lastly, θ_d is the Bragg angle.

$$n\lambda_L = 2\Lambda \sin(\theta_d) \tag{2.7}$$

The reflection of this Bragg condition is visualized in Figure 2.10. In this figure there is the incident beam that will travel through the crystal. The black lines are the diffraction grating that will be moving with a certain speed, which means we have a dynamic diffraction grating. The dynamic diffraction grating is being generated by the acoustic wave propagating through the crystal. This acoustic wave induces a period modulation of the reflective index, which is forming this dynamic diffraction grating. The incident beam will scatter off this diffraction grating with an angle $2m\theta_d$. This m represents the different orders of scattering. In this case, m can be 1 or 0. When rewriting Formula 2.7 we get that the scattering angle is equal to $2m\sin^{-1}(\frac{n\lambda_L}{\Lambda})$. Here it can be seen that this angle is dependent on the refractive index. This means that changing the refractive index will change the reflection of the incident beam.

2.8.2. CONTROLLING THE AOM

In Figure 2.10, the configuration of the crystal can be seen. The AOM circuit will pass an RF wave into the crystal. The transducer will convert these RF waves into acoustic waves that will travel through the crystal. This will create the dynamic diffraction grating as explained before. These transducers will be made out of piezoelectric materials [21], [22].

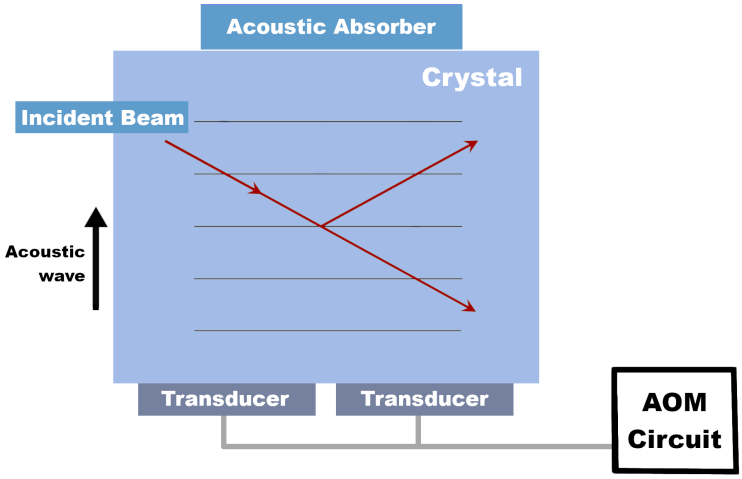

Figure 2.10: The AOM crystal that shows the connection of the piezoelectric transducer and AOM circuit

These electrical signals need to be in the form of an RF signal. The RF signals will be generated by the AOM driver. The AOM driver and its components can be found in Figure 2.11. As inputs, we have two signals, MOD and DC. MOD is a modulation signal that will simply tell us on or off. There will also be a DC input that will be converted into an RF signal. The first component of the driver will be a voltage controlled oscillator (VCO). This VCO will provide an RF output, and its frequency will be based on the applied voltage. When the modulation signal is off we will have no RF output. The next component in line will be the voltage variable attenuator. This component will attenuate the signal that comes from the VCO, and, as the name already implies, this attenuation is variable. Lastly, we will have an amplifier. It is common practice to distinguish the amplifier from the other components. This is because we want to guard the amplifier from the heating of the other components. Also, having a shorter connection between the amplifier and AOM will minimize any loss of signal.

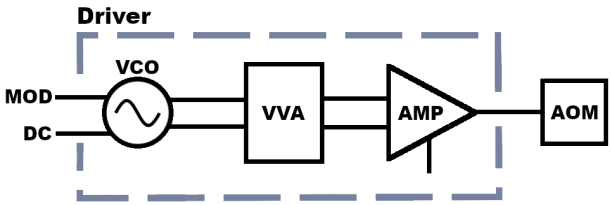

Figure 2.11: Schematic of the driver circuit

In the driver circuit there are variable components. This is done because the RF signal that the AOM must receive will be different for different laser power and wavelength. Having a good configuration of these components is important to minimize damage to the crystal.

3

REQUIREMENTS

The goal is to measure the Rabi oscillations. With these Rabi oscillations, we can control and characterize the NV centers. This can increase the sensitivity and give better measurements.

- **Room-temperature**- The measurements must be able to perform at room-temperature (293K).
- **Measurement setup**- The Rabi oscillation must be measured with the current measurement setup and what is available.
- **Timing resolution** - To have a high enough resolution in the oscillation, the pulse length should be able to be increased in steps of $2ns$.
- **Background noise** - The measurements must be able to distinguish background noise.
- **Oscillations** The measured oscillations must resemble a decaying cosine wave. Similarity will be measured with cross-correlation, which should be above 70% to have a strong enough correlation.

During the experiments, the AOM broke down, and thus we needed to change the requirements because of this. The requirements above still hold, but new ones were appropriate.

- **Stability** - The AOM driver must be able to output a stable RF signal of $110MHz$ and must be controlled by the modulation signals.
- **Compatibility** - The newly designed AOM should be compatible with the driver that is used.
- **Reflection** - The AOM circuit should have an efficiency of more than 96% to avoid distortion in the signal and damaging the driver, which means the reflection coefficient must be less than 0.04.

4

MEASUREMENT PROCEDURES

4.1. MEASUREMENT SETUP

In Figure 4.1, the laser setup can be seen. Directly after the laser, the beam reflects from a mirror that works in combination with a second mirror. The two steering mirrors are used to precisely position the beam before it enters the AOM. Between the two mirrors there is a polarization beam splitter (PBS) to ensure that only light with a well-defined linear polarization enters the diamond.

After the second mirror, the beam enters the AOM. The diaphragm after the AOM is positioned in such a way that only one harmonic from the AOM can pass through. When this AOM is turned on, this harmonic will be present, otherwise not. This allows for turning the laser on or off. Then there is a beam expander that takes a collimated beam of light and expands its width, which is needed for a better focus.

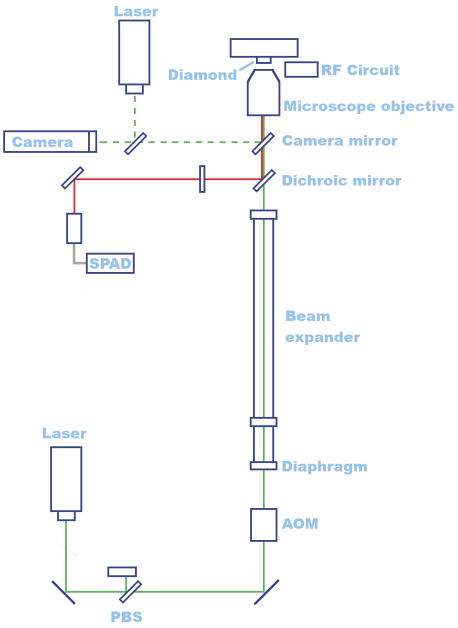

Figure 4.1: Schematic of the measurement setup that is used for all the experiments.

The dichroic mirror is used to reflect the right light returning from the sample to the SPAD while letting the green laser pass. The camera mirror is used in combination with

a camera and a second laser to check if the SPAD is actually focused on the same point in the sample where the green light arrives. The camera is also used to check the quality of the green laser and if it is able to turn on and off properly.

The microscope objective is used to tightly focus the green laser with very small adjustments and increase the optical intensity due to its high numerical aperture. For the same reason, it can also better collect the emitted fluorescence.

Lastly, the RF circuit just beside the diamond sample provides the RF radiation that is needed for the Rabi oscillations.

4.2. CONTROLLING THE SETUP

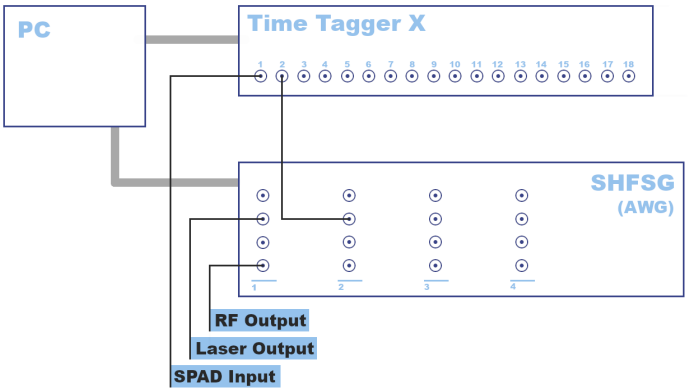

Figure 4.2: Overview of the devices used and their connections to the setup

The AOM, the RF circuit, and the SPAD need specific and accurate control. Three devices are used for this: a PC running Python code, the Swabian Instruments Time Tagger X [23] and the Zurich Instruments SHFSG+ [24]. The SHFSG+ is an Arbitrary Wave Generator (AWG), which is used to create precisely defined, user-specified voltage waveforms over time. The Time Tagger is to count the pulses coming from the SPAD between two triggers. The Time Tagger and AWG are connected to each other and to the setup via SMA cables, and the PC is connected to both devices via Ethernet.

The AWG has multiple signal channels. For each channel, there are four different connections: Trig, Mark, Aux In and Out. For this project, only the marker (Mark) output and analog output (Out) will be used. The marker output is a digital output, and the analog output is used for RF signals. [25]

The output of channel 1 is used by the RF circuit and is responsible for turning the right

frequency on at the right moment. The marker output of channel 1 is connected to the driver of the AOM and can modulate the driving signal and in that way control the laser. The marker output of channel 2 is used as a trigger for the Time Tagger. The Time Tagger can be initialized to only count between the rising and falling edge of this trigger pulse [26].

On the computer, LabOne and the Zurich toolkit Python library are used to control the AWG [27]. All the device settings can be initialized with the code, and then a wave sequence can be sent to the memory of the machine. The code that runs on the AWG is written in SeqC, which is a custom version of C. In this code, wave functions can be defined and played after each other. This way, all timing will be handled by the device itself and not by the Python code, which would not be accurate enough.

4.3. PROPOSED METHOD

In Section 2.7, different methods for measuring Rabi oscillations have been discussed. The method that uses optomechanical control gives more control over the qubits. However, at the moment the measurement setup cannot handle this experiment since the diamond sample does not have a ZnO substrate around it. Moreover, this method will not give more accurate results, it is just useful for better control of the qubits. This means that the first method would be more of a logical choice and can be done without any alterations to the current setup.

The duration of different parameters of the measurement can be seen in Table 4.1. They are based on [28], but will be fine-tuned for this specific setup and diamond sample after the first measurements. The padding is added on both sides of the RF pulse, so the laser is off for the duration of the RF pulse plus 2 μs. The RF pulse duration is swept from 0.5 to 4 μs with steps of 0.002 μs. The sweep will be done 250 times and averaged to get better data, as there is a lot of randomness in the amount of photons that will be detected. Between every sequence there is a delay of 0.2 seconds while the laser is on to let the spin system reset.

There are two ways in which the measurement will be done: only measuring the photons after the RF pulse, or also measuring it before and then taking the difference to remove the noise. The second method will likely provide better results. [12]

Table 4.1: Timing of the measurement

Parameter	**Duration** [μs]
Read out laser pulse	5
RF pulse	0.5-4
Padding	1

All used settings on the machine are shown in Table 4.2 and 4.3. The frequency of the output of the AWG can only be a product of 200MHz, but it can be modulated with other oscillators to reach the desired frequency of 2.87GHz. The center frequency of both

channels is set to 2.8GHz, and on the first channel it is also modulated with an oscillator of 70MHz. For this to work, sine generation needs to be turned on, which consists of two parts, both of which are needed: In-phase (I) and Quadrature (Q). Both channels have synchronization turned on so that the wave sequences start at the same moment every time they are run.

Table 4.2: SHFSG channel 1 settings

Label	Setting / Value / State
synthesizers[0]/center/frequency	2.8e9
sgchannels[0]/output/on	True
sgchannels[0]/output/range	0
sgchannels[0]/sines[0]/i/enable	True
sgchannels[0]/sines[0]/q/enable	True
sgchannels[0]/oscs[0]/frequency	0.07e9
sgchannels[0]/synchronization/enable	True
sgchannels[0]/marker/source	awg_trigger0
sgchannels[0]/awg/outputamplitude	1

Table 4.3: SHFSG channel 2 settings

Label	Setting / Value / State
synthesizers[1]/center/frequency	2.8e9
sgchannels[1]/output/on	True
sgchannels[1]/output/range	0
sgchannels[1]/synchronization/enable	True
sgchannels[1]/marker/source	awg_trigger0
sgchannels[1]/awg/outputamplitude	1

In the code segments below is the code that is sent to the machine to control channels 1 and 2. Firstly, different waveforms are made, all of which are just constantly on or off in this case. Then the waves are played, and the marker output is turned on or off in between the waves. The sample rate is 2GHz so every time value (in seconds) needs to be multiplied by that. PULSE_LENGTH is a variable that is set to different values ranging from 0.5 to 4μs every time the sequence is sent to the machine. The setTrigger function sets the marker output on or off, the playWave function plays a previously defined wave, and the waitWave function waits for the previously started wave to end before continuing. The waves on channel 1 modulate the RF output. When $microwave$ is played, the RF output will be on, otherwise it will be off, as it is the only wave consisting of ones. For channel 2, the waves are only there to handle the delays between the trigger switches.

SeqC Code Channel 1

```
wave padding = zeros(2000);
wave microwave = ones( PULSE_LENGTH * 2e9 );
wave read_out = zeros(10000);

setTrigger(0);
playWave(1, padding);
waitWave();
playWave(1, microwave);
waitWave();
playWave(1, padding);
waitWave();
setTrigger(1);
playWave(1, read_out);
```

SeqC Code Channel 2

```
wave read_out_delay = zeros((2e-6 +  PULSE_LENGTH ) * 2e9));
wave read_out_marker = zeros(10000);

playWave(1, read_out_delay);
waitWave();
setTrigger(1);
playWave(1, read_out_marker);
waitWave();
setTrigger(0);
```

5

AOM Design and Testing

For measuring the Rabi oscillations, an AOM is an essential part of the measurement setup. However, during one of the experiments, the AOM that was used failed, which resulted in a delay. After long consideration, we had decided to try and fix the AOM ourselves. Firstly, we will look into the commercially bought AOM and driver and how they operate together. After this we will go in depth about the failure of the device. Then we will try to fix the AOM, and we will look into the crystal and a new design for the circuitry of the AOM.

5.1. Commercial AOM and driver

For the experiments, a commercial AOM had been bought. For this AOM to work an RF driver is needed. This RF driver is necessary to create an RF wave to let the AOM operate under the right frequency.

5.1.1. AOM

The AOM that is used is the ISOMET M1205-T110L-1 [29]. The AOM consist of an internal matching circuit to match it to the RF driver and a TeO2 crystal. The internal matching circuit can be seen in Figure 5.7. The resistors in the circuit are variable resistors, which are used to configure the circuit to the crystal. In the circuit, V_{in} is the input signal that comes from the driver, and V_{out} is the signal that goes into the crystal.

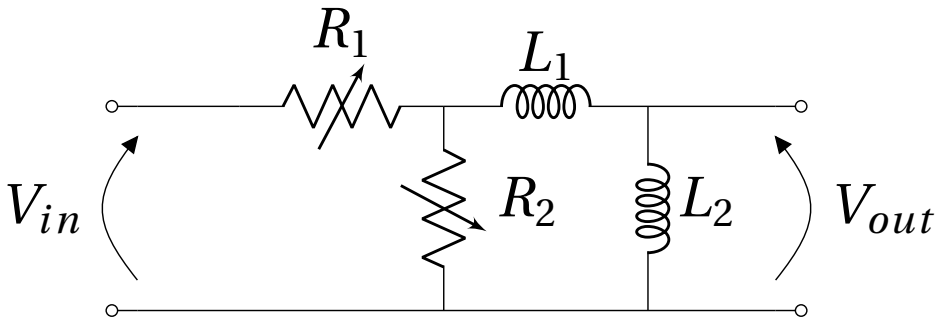

Figure 5.1: AOM internal circuit

5.1.2. RF DRIVER

To generate the RF input signal of the AOM circuit, the Isomet 523F-2 driver [30] is used. This driver converts a DC signal to an RF signal that can be used by the AOM. This driver also has a modulation input. This modulation signal makes it possible to nullify the RF signal by pulling it to the ground. The driver has an attenuator to adjust the output power, which must be configured based on the AOM that is being used. The output power of the driver plays a big role in the behavior of the crystal, since the reflective index of the crystal depends on the mechanical strain, which is directly proportional to the power of the RF input signal (Equation 2.6).

5.1.3. FAILURE

During one of the experiments, the AOM broke down. Since the AOM is a crucial component for measuring Rabi oscillations, the project came to a halt. It is important to analyze what went wrong. In Figure 5.2, the circuit can be seen. The resistor to the right blew up, which means there is an open circuit and no connection anymore. Also, the rightmost connection to the crystal is broken. This means that no acoustic waves can be generated.

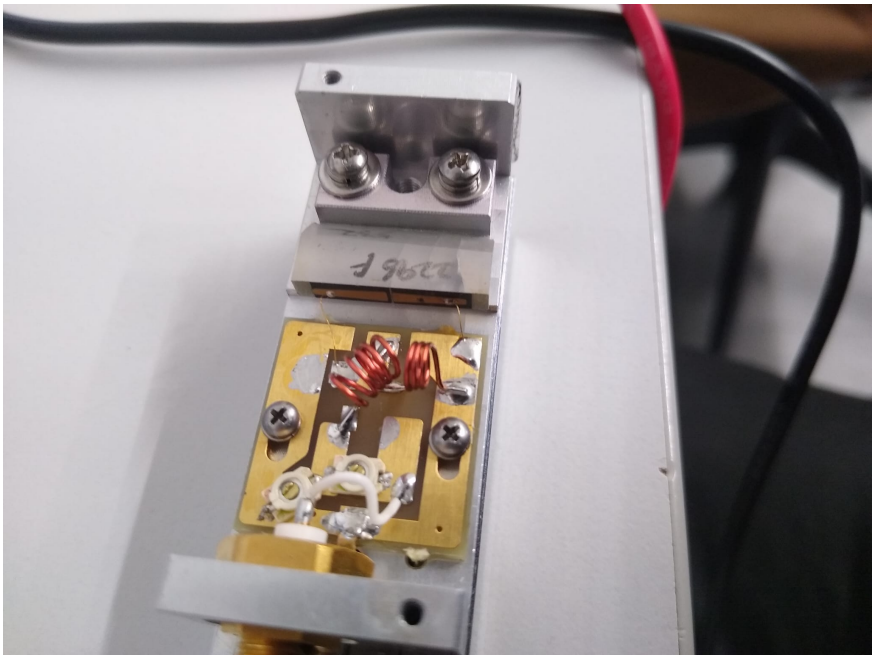

Figure 5.2: The internal matching circuit of the commercial AOM

The components were not the only problem, as can be seen in Figures. 5.3. In these figures cracks in the crystal can be seen, which is problematic when working with very sensitive components. The cracks in the crystal can cause a bad refraction, and they could also affect the acoustic waves that will be traveling through the crystal.

(a) The cracks in the crystal seen from the side

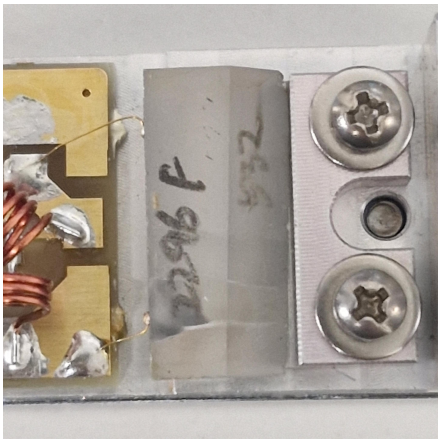

(b) The cracks in the crystal seen from above

Figure 5.3: Images that shows the cracks in the crystal that were noticed after the AOM failure.

CRACKING OF CRYSTAL

An external expert was consulted over the malfunctioning of the AOM. The expert suggested that the crystal damage may have resulted from a modulation signal that was too fast, which made the crystal unable to relax between the cycles and unable to handle the stress. This cracking of the crystal could lead to a change in impedance or altering the acoustic wave propagation. Both changes will result in reflection in the circuit, which can lead to heat or breaking down of components.

WRONG ATTENUATION

Another explanation could be that the attenuation of the driver was wrongly configured. This results in too much power that is being transmitted to the AOM circuit. This power can damage the components and create cracks in the crystal. This can also explain why the AOM was heating up when it was used for a while.

5.2. TESTING THE CRYSTAL

Since the previous AOM failed, it was necessary to create a custom AOM to continue the experiments. The only part of the AOM that was kept was the TeO2 crystal. This crystal still contained cracks, but this was the only way to continue the project. To test the crystal, two copper plates were attached to the crystal, as can be seen in Figure 5.4. An ideal situation would be to have a piezoelectric material between the copper and crystal that behaves like an inducer as described in section 2.8.2. This was, however, not possible due to limited resources, but the TeO2 crystal can behave piezoelectrically [31].

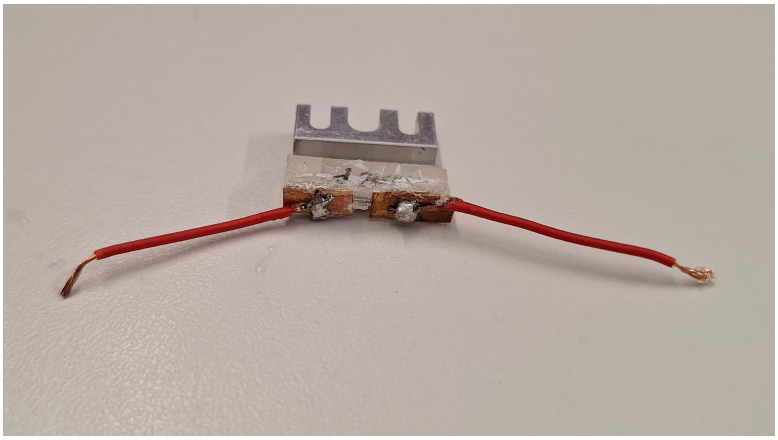

Figure 5.4: The setup which we used for testing the piezoelectric effect and measured the impedance, which is used for creating a matching circuit.

5.2.1. PIEZOELECTRIC EFFECT

Firstly, we needed to make sure the crystal was still behaving piezoelectrically. This can be tested by measuring the piezoelectric effect. This means creating mechanical vibrations from electrical signals or creating electrical signals from mechanical vibrations.
If the crystal were working accordingly, an electrical signal would be observed when a

force is applied. In Figure 5.5, the result of this experiment can be seen. In the figure, a sinusoidal wave that has been distorted by a peak can be seen. This peak was the electrical signal that was created by the crystal when a force was applied. This shows that the crystal is showing a piezoelectric effect, which means it can be used for further testing.

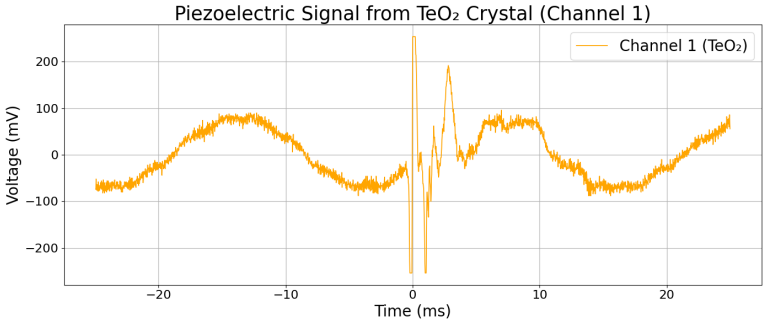

Figure 5.5: The piezoelectric effect of the TeO2 crystal, that was created by applying force to the crystal

5.2.2. IMPEDANCE OF THE CRYSTAL

To create a circuit for the custom AOM, the impedance of the crystal must be known. This impedance can be measured with the help of a Vector Network Analyzer (VNA). The VNA that will be used is the LiteVNA [32]. With a VNA, it is possible to measure the transmission coefficient of a circuit. In this case we have a 1-port network with only 1 scattering parameter, S. With this scattering parameter, the impedance of the piezo element can be calculated with Equation 5.1. Notice that $S = \Gamma$. For the VNA that has been used, the characteristic impedance Z_0 is equal to 50Ω.
Measuring the scattering parameter with the VNA resulted in $S = -0.668 - j0.721$. This measurement has been done at a frequency of $110MHz$, since this is the frequency of the driving circuit. This concludes in an impedance of $Z_{crystal} \approx 0.51 - j21.83\Omega$.

5.3. DESIGNING THE MATCHING CIRCUIT

It is important to match the input impedance of the AOM to the output impedance of the driver to maximize power transfer and minimize signal reflection. Maximum power is delivered to a load when the load impedance is the complex conjugate of the source impedance. However, most source impedances in RF systems are purely real, so the load should also be purely real, and the real parts need to match.

Reflections of the signal cause standing waves, which can result in power loss and distortion of the signal. The degree of signal reflection Γ can be calculated with 5.1, where Z_L is the impedance of the load and Z_0 the characteristic impedance of the source or transmission line. It can be seen that the reflection is minimal when Z_L and Z_0 match.

$$\Gamma = \frac{Z_L - Z_0}{Z_L + Z_0} \tag{5.1}$$

5.3.1. L-NETWORKS

An L-network is one of the most simple types of matching circuits used to match two real impedances, and it consists of two reactive components, either inductors or capacitors, arranged in an "L" configuration. In an L-network, the two components work together to transform the resistance and cancel the reactance caused by the other.

The first step is to use a reactive component to cancel the imaginary part of the load impedance, because the L-network only works for real impedances. The imaginary part is negative in this case, which means that the load is conductive. An inductor with the opposite impedance is needed in series to cancel it. The reactive part of the load is −21.83. The inductance needed is then calculated to be 31.6 nH, see Equation 5.2.

$$L = \frac{X}{2\pi f} = \frac{21.83}{2\pi \cdot 110 \cdot 10^6} = 31.6[nH] \tag{5.2}$$

There are four basic L-network configurations, see Figure 5.6. There are two high-pass circuits and two low-pass, dependent on which component is in parallel and which is in series. The order of the components also matters if the load resistance is smaller or larger than the source resistance. To increase the load resistance to match the source, a reactive shunt component can be added to the load, which increases the real part of the impedance. After that, the newly added reactance can be canceled by a series component. To decrease the load impedance, first a series reactance is added, which introduces an imaginary component without changing the resistance. Then a shunt reactance is added, which transforms the complex impedance to a lower value. In this case, the resistance of the load is only 0.51 Ω, which is lower than the source impedance, which is 50 Ω. As this is a high-frequency circuit, DC voltage needs to be blocked, so circuit (D) is the best choice as it is a high-pass filter suited for when $R_L < R_S$.

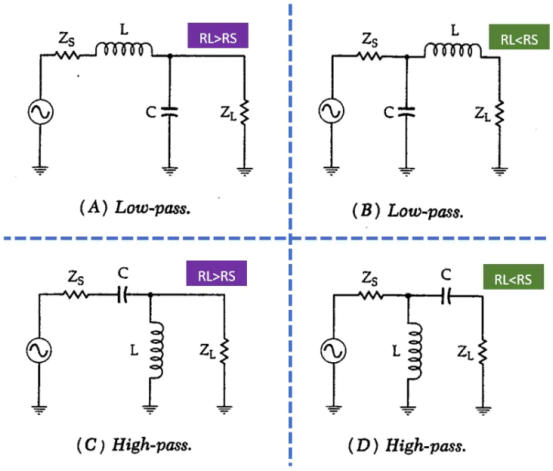

Figure 5.6: Four different types L-shaped matching networks [33]

5.3.2. Q FACTOR

The next step is to calculate the Q factor of the matched circuit. The Q factor, or Quality Factor, is a measure of how much reactive energy is stored in relation to how much real power is dissipated (Equation 5.3). This Q factor can be useful for designing matching circuits, as it indicates how far apart the source and load impedances are. Moreover, the Q factor can also tell something about the created network: low Q factors mean higher losses and more noise, but at the same time a larger bandwidth, while high Q factors will result in the opposite.

$$Q = \frac{X}{R} \tag{5.3}$$

There are two Q factors in an L-network, one for the component that is either in series with the load or in series with the source (Q_s), and one for the component that is parallel (Q_p). These two Q factors are set equal to each other so that the reactances resonate together and match the impedance transformation, because at resonance, the reactances match each other and cancel out. So in the end there's only one Q factor that creates a matched condition. Because there is only one possible Q factor, the bandwidth of the matching circuit is also fixed.

5.3.3. RESISTANCE MATCHING

In general, all L-network circuits can be split into two parts that must have the same resistance. The first part consists of a resistance with a reactance in parallel, and the other part of a resistance and reactance in series. Setting the impedance of these equal to each other results in Equations 5.4 and 5.5.

$$R_s + jX_s = R_p || jX_p = \frac{jR_pX_p}{R_p + jX_p} = \frac{jR_pX_p}{R_p + jX_p} \cdot \frac{R_p - jX_p}{R_p - jX_p} \tag{5.4}$$

$$R_s + jX_s = \frac{R_pX_p^2}{R_p^2 + X_p^2} + j\frac{R_p^2X_p}{R_p^2 + X_p^2} \tag{5.5}$$

Equation 5.3 only works for reactance in series with a resistance, but for parallel reactance it works differently. The real and imaginary parts of both sides of Equation 5.5 can be used to get the correct ratio transformation as seen in Equation 5.6, which results in two separate equations for the Q factor (Equation 5.7). In this case, the source impedance is taken as parallel with the inductor, and the capacitor and load impedance are in series.

$$Q = \frac{X_s}{R_s} = \frac{\frac{R_p^2X_p}{R_p^2+X_p^2}}{\frac{R_pX_p^2}{R_p^2+X_p^2}} = \frac{R_p^2X_p}{R_pX_p^2} = \frac{R_p}{X_p} \tag{5.6}$$

$$Q_p = \frac{R_p}{|X_p|} = \frac{R_S}{|X_L|} \qquad Q_S = \frac{|X_s|}{R_s} = \frac{|X_C|}{R_L} \tag{5.7}$$

At resonance, the reactance of both parts of the circuit will be equal, as later on the same Q factor will be used for both of them to calculate the component values. So only the real part of the equation is kept, and Equation 5.3 is used to substitute X_p for R_p/Q_p. This results in Equation 5.8.

$$R_s = \frac{R_p X_p^2}{R_p^2 + X_p^2} = \frac{\frac{R_p^3}{Q_p^2}}{R_p^2 + \frac{R_p^2}{Q_p^2}} = \frac{\frac{R_p^3}{Q_p^2}}{R_p^2\left(1 + \frac{1}{Q_p^2}\right)} \tag{5.8}$$

Then the relevant value names are filled in and the expression is simplified to Equation 5.9 and 5.10.

$$R_L = \frac{\frac{R_S^3}{Q_p^2}}{R_S^2\left(1 + \frac{1}{Q_p^2}\right)} = \frac{\frac{R_S}{Q_p^2}}{1 + \frac{1}{Q_p^2}} \tag{5.9}$$

$$R_S(1 + Q_p^2) = Q_p^2 R_L \Rightarrow R_S + R_S Q_p^2 = Q_p^2 R_L \tag{5.10}$$

Solving this for Q results in Equation 5.11.

$$R_S = Q_p^2(R_L - R_S) \Rightarrow Q_p^2 = \frac{R_S}{R_L} - 1 \Rightarrow Q_p = \sqrt{\frac{R_S}{R_L} - 1} \tag{5.11}$$

This gives a formula for Q_p, and then the Q factor of the series part of the circuit, Q_s, is set to be equal to Q_p so that the reactances will resonate. Then the actual resistances of the source and load are filled in to get the Q factor of the circuit (Equation 5.12). For the load, only the resistance is used because the reactance is already canceled by the inductor that was added. The Q factor of the circuit is 9.85, which is quite high and indicates that this is a narrow-band circuit.

$$|Q_S| = |Q_P| = \sqrt{\frac{R_S}{R_L} - 1} = \sqrt{\frac{50}{0.51} - 1} = 9.85 \tag{5.12}$$

5.3.4. COMPONENT VALUES

Then, to get the values of the components that need to be used, firstly, Equation 5.7 is used to get the reactances (Equation 5.13), and then the formulas for capacitance and inductance are used to get the actual component values (Equation 5.14).

$$|X_C| = R_L \cdot Q = 5.02\ \Omega \qquad |X_L| = \frac{R_S}{Q} = 5.08\ \Omega \tag{5.13}$$

$$C = \frac{1}{2\pi f |X_C|} = 288\ pF \qquad L = \frac{|X_L|}{2\pi f} = 7.34\ nH \tag{5.14}$$

5.3.5. ABSORPTION

The calculated capacitance will be in series with the inductance of 31.6 nH that cancels the reactance of the load, so they can be combined into one component. This component has a positive reactance, so the part will be an inductor (Equation 5.15).

$$X = 21.83 - 5.02 = 16.81 \qquad L = \frac{X}{2\pi f} = 24.3\ nH \tag{5.15}$$

The resulting circuit can be seen in Figure 5.7 and the L-network consists of two inductors.

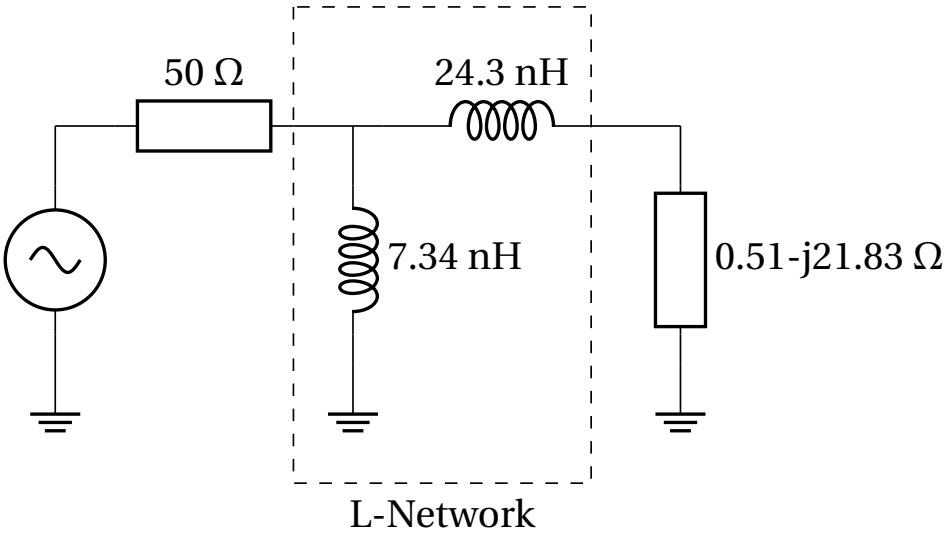

Figure 5.7: AOM internal impedance matching circuit

5.3.6. SIMULATION

The circuit was simulated in Python to get the total input impedance, which turned out to be $50 + 0j$, which is exactly the output impedance of the source.

Equation 5.1 is used to calculate the reflection coefficient Γ for frequencies between 100 and 120 MHz. This value can also be seen as the return loss, as the power that is reflected can't be used. The result is plotted in Figure 5.8, and it can be seen that the dB loss goes to minus infinity at 110 MHz.

For this simulation, the impedance of the crystal was assumed to be 0.51 - j21.83Ω. However, this was measured at 110MHz, and the simulation goes from 100 to 120 MHz, so this can cause some inaccuracy in the shape of the graph.

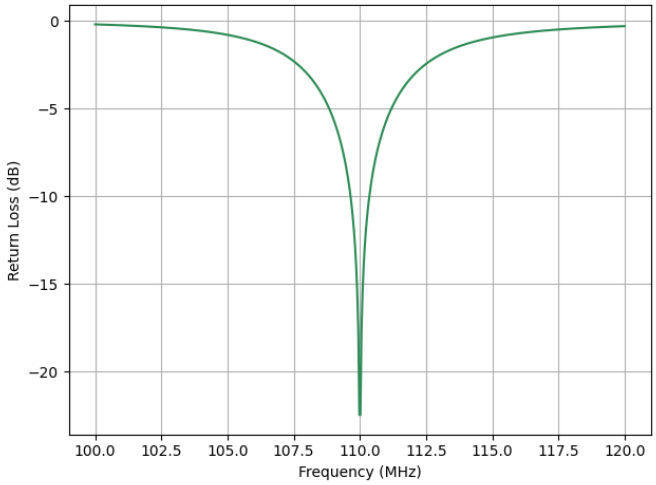

Figure 5.8: Return loss of the impedance matching circuit

The magnitude and phase of the input impedance per frequency are plotted in a Bode plot in Figure 5.9. The circuit behaves as a narrow-band band-pass filter. In theory, this circuit should function properly.

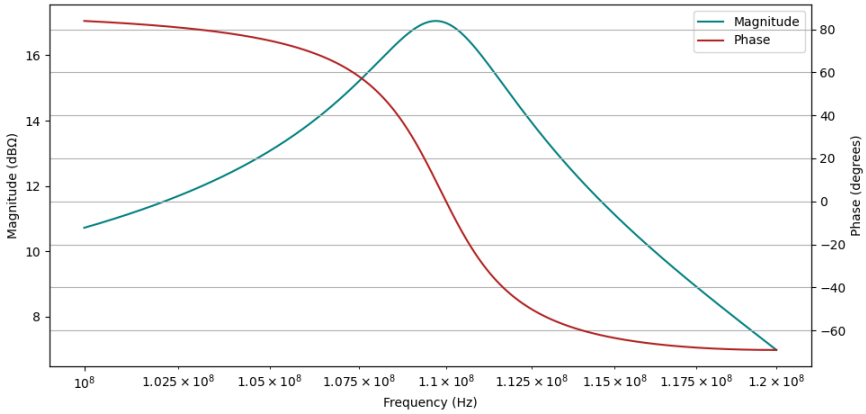

Figure 5.9: Simulated bode plot of the input impedance

5.4. TESTING THE CUSTOM BUILT AOM

Now that everything has been tested, the circuit can be built. The RF coils from the commercial AOM were used for the inductors. The VNA was not accurate enough to measure the impedance of these coils. They were estimated to have an impedance of 60 and 30 nH based on the dimensions [34]. In the end, two potentiometers were added to the circuit in order to make small adjustments to compensate for the wrong inductor

impedances (Figure 5.10). The potentiometers, R_s and R_p, are 0 to 100 Ω.

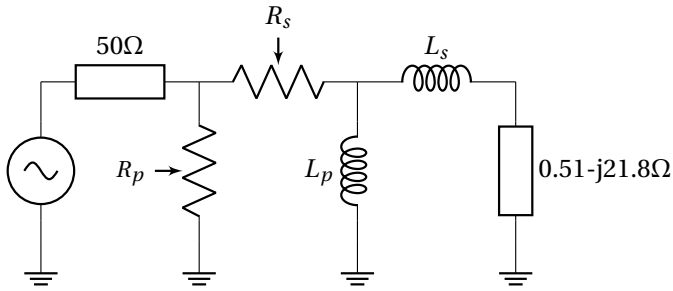

Figure 5.10: AOM internal impedance matching circuit

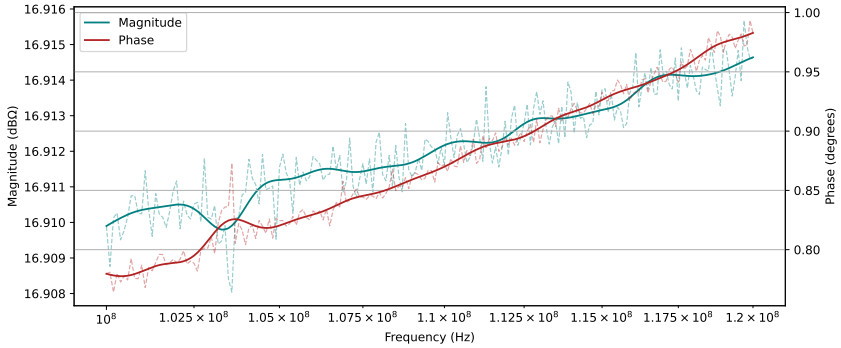

Figure 5.11: Measured Bode plot of the input impedance

A VNA was again used to measure the total impedance of the circuit in combination with the crystal at a frequency range of 100 to 120 MHz. At 110MHz, the impedance is 49.103 + j0.747 Ω, which is close to just 50Ω and the reflection coefficient is -0.00899 + j0.00761, of which the absolute value is 0.0118. Using Equation 5.16 will result in an efficiency of 99.986% for the whole circuit.
The shape of the plot doesn't resemble the simulated Bode plot because of the newly added resistors. A big downside of the resistors is that they consume significantly more power than just reactive components, but they did end up getting a lower reflection coefficient, which is more important because more power can always be provided by the driver.

$$Efficiency = (1 - |\Gamma|^2) * 100\% \tag{5.16}$$

In Figure 5.12, the circuit can be seen. From the figure it is clear that the green laser does not fully pass through the crystal. This resulted in a distorted laser that no longer converges to a defined point. When the RF driver was supplying an RF wave to the circuit, no diffraction could be seen. This could be due to the cracks that are preventing the acoustic waves from traveling through the crystal. Another explanation would be that no acoustic waves are generated even though the piezoelectric effect has been observed. However, this piezoelectric effect could be too small because no transducers were used between the copper plates and crystal.

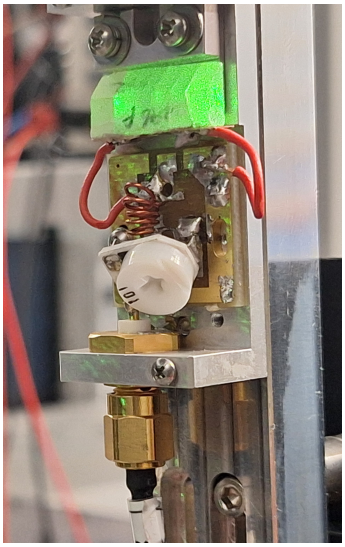

Figure 5.12: The custom-built AOM with a green laser passing through the crystal. It can be seen that the laser is not really passing the whole crystal.

6

RESULTS

In the following section, the results will be presented. All the experiments that have been done were with the commercially bought AOM. The AOM was still working during these experiments. However, this AOM was heating up during the experiments, which influenced some of the measurements.

6.1. TESTING THE MEASUREMENT SETUP

To test the measurement setup, we can check if the AWG is outputting the signals as we anticipated. This can be done by connecting the AOM to an oscilloscope. Then it can be seen if the timing will be the same as discussed in Section 4.3.

6.1.1. AWG

For this measurement, the RF frequency was set to 600MHz, as the oscilloscope is rated for frequencies up to 200MHz, so frequencies that are way higher than that can't be visualized, and 600MHz is the lowest the AWG can output. As a test, an RF pulse of 0.5 μs was chosen. It can be seen that all outputs are correct. The channel 1 marker turns the laser off for 2.5 μs, which is equal to the RF duration plus padding on both sides of 1 μs. The channel 2 marker going to the Time Tagger is on before the pulse for 5 μs and after for 5μs. This means that the AWG is correctly putting out all the signals, and we can connect it to the other devices.

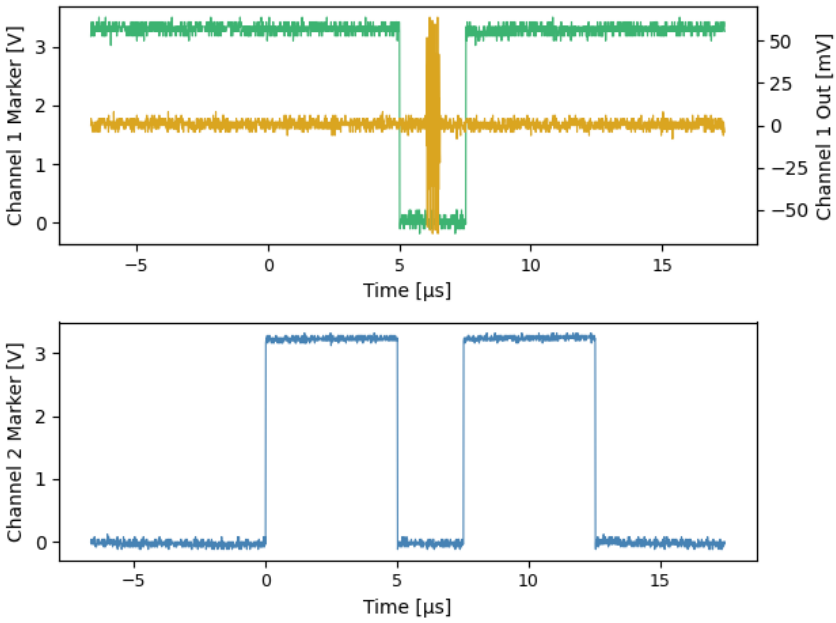

Figure 6.1: Oscilloscope measurement of the AWG output

6.1.2. ODMR

As could be seen in the previous subsection, all the control signals are correctly being sent by the AWG. This, however, tells nothing about the devices specifically. To know if most devices are working properly, an ODMR measurement as described in Section 2.4 can be done. This measurement tells us if the RF circuit can be driven successfully. For this measurement a sweep from $2.855GHz$ to $2.885GHz$ has been done. In Figure 6.2, the result of this measurement can be found.

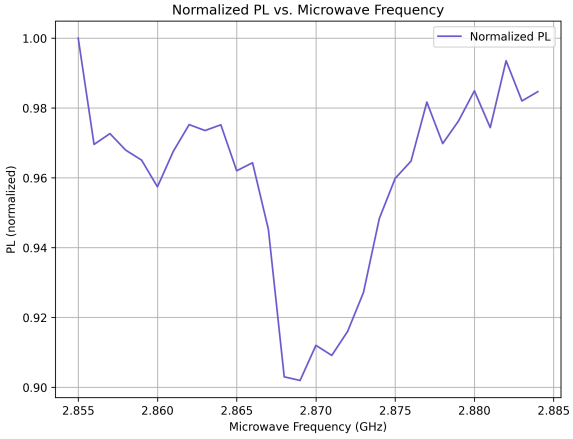

Figure 6.2: ODMR measurement without a magnetic field

In this figure a clear dip around $2.87GHz$ can be seen, which means that the RF circuit is being driven by the AWG successfully. This measurement also shows that both the time tagger and laser can be controlled in the correct manner.

6.2. RABI OSCILLATIONS

For measuring the Rabi oscillations, the method discussed in Section 4.3 will be used. The sweep was done for a total of 250 times to try and get enough data. For this measurement, the SPAD was only measuring after the RF pulse. To extract the Rabi frequency from the data, we can fit the data onto an oscillating function that can be seen in Figure 6.1, [35]. This function will be of the same form as the Rabi oscillations that will be measured. For this reason we can try to fit the data of the measurement onto this function. The function has the 4 different constants, a_R, b_R, c_R and d_R. These constants mean the amplitude, decay time, Rabi frequency and phase difference. This amplitude says something about the contrast between the spin states. This means when there is a high amplitude a lot of the qubits will be oscillating between the spin states and a lower amplitude means that less qubits are oscillating between the spin states.

$$f(\tau) = a_R \cdot (1 - e^{-\tau/b_R} \cdot cos(c_R \cdot \tau + d_R)) \tag{6.1}$$

The function will be fitted onto the data that has been measured. To get a good plot, an initial guess must be done. To have a good guess, the data will be smoothed out. In Figure 6.3, the original data and the smoothed data can be seen. From this smoothed data we can guess the amplitude to be around 2 and the Rabi frequency to be around $6MHz$. The decay time can be guessed with the help of the following paper [36]. In this paper it states that at room temperature diamond samples with a $10ppm$ will have a decay time of $2-39\mu s$. The sample used in this project has around $6-7ppm$, thus a guess of $25\mu s$ for the decay time seems appropriate. The phase difference will be guessed at 0. This phase difference can be important because the measurement starts at $0.5\mu s$ and not 0. When fitting the data onto the function with this initial guess, it resulted in a damped cosine function that can be seen in Figure 6.3.

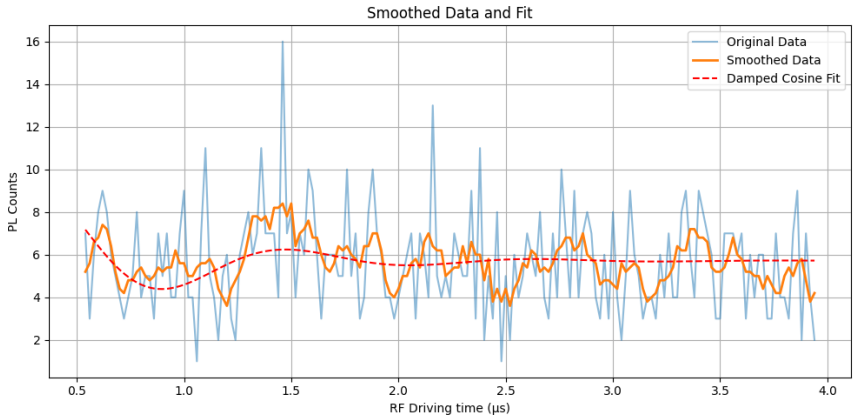

Figure 6.3: Smoothed curve of the Rabi oscillations for driving times from $0.5\mu s$ to $4\mu s$, with a repetition of 250 times.

The initial guess and the retrieved parameters can be found in Table 6.1. The results

show a lot higher decay time, but this decay time can still be in a plausible range. The same goes for the other values.

Table 6.1: Initial Guesses vs. Fitted Values for Damped Cosine Model

Parameter	Description	Initial Guess	Fitted Value
a_R	Amplitude	2	5.714
b_R	Decay time (μ s)	25	63.037
c_R	Rabi Frequency (MHz)	6	5.432
d_R	Phase Offset (rad)	0	1.135

This fitting is based on several estimations. Therefore, it is essential to calculate the correlation between the original data and the fitted model. This can help determine if the measurement data aligns with the fitted model and how close the match is. In Chapter 3, it states that the correlation should be above 70%. The correlation that came out of this plot was 15.795%, which does not come even close. Thus it cannot be stated that the Rabi oscillations has been measured successfully. However, the parameters in Table 6.1 are very plausible, but since the correlation is this low, we can't conclude this with certainty.

This unsuccessful measurement could be due to the photoluminescence count, which is extremely. It could be that during the experiment no real photoluminescence was measured, only dark counts. This could be due to bad alignment of the laser. Due to the measurement having a low photon count, no clear Rabi oscillations can be extracted from the graph. And more measurements must be done to have better insights.

7

DISCUSSION

During the course of this thesis, there were multiple challenges that needed to be overcome. In this chapter we will look at these challenges and how they have been solved or can be prevented for further experiments.

Optical Alignment: To get an optimized measurement, a high photon count is needed. This high photon count is needed because the measurement will be really short. The highest photon count was achieved by aligning the laser perfectly with the NV diamond sample. This, however, proved to be a difficult task. The alignment could be checked with a camera and corrected by turning all the optics. This aligning could only be done when nothing else was happening in the lab, but the lab was during our time extensively used, which led to limited alignment time.

Lab oscilloscope: The oscilloscope that was provided in the lab proved to be a headache. The oscilloscope had only one channel that gave correct data, all the other channels were off or had a lot of noise in the system. All the signals that needed testing were of higher frequencies, which could not be measured by this oscilloscope, since its range goes up to $100MHz$. To solve these issues, we borrowed an oscilloscope from another lab.

Degrading photon count: During longer experiments, the total photon count degraded over time. This resulted in inaccurate measurements and measurements that needed some after-processing to get clear plots. This problem had been occurring during other measurements as well. A possible explanation would be the AOM that was warming up. When the AOM was warming up, it could result in a different laser output, which would excite fewer NV centers. This could be an explanation of the degrading photon count.

AOM: During one of the experiments, the commercially bought AOM failed. This resulted in a long time delay and discussion for the next step. It was also the only thing that prevented us from measuring the Rabi oscillations. As a solution, we tried creating our own custom-built AOM. But the research group is also looking at alternatives: a

pulsed laser or fiber-coupled AOM. This will also create a better output pulse than the commercially bought AOM could ever achieve.

VNA: To measure the impedance of the crystal and the designed matching circuit, the VNA lite was used. During the measurement the impedance, the VNA was very instable, even after calibrating it. Due to this, it was not possible to measure the impedance of the small inductors that were used. This resulted in a lot of approximating when building the circuit. No other VNA was available, which meant we were stuck with using this VNA.

Custom built AOM: Due to the limited resources that could be used, we could not create a good transducer for the AOM. After testing the crystal, we saw no diffraction happening. This could be due to the fact that the mechanical signals that were traveling through the crystal did not have enough power. An explanation for this would be that no piezoelectric transducer was used, which was not available to us. Another reason could be that there were too many cracks in the crystal, which prevented these waves from traveling through.

8

CONCLUSION AND OUTLOOK

The original goal of measuring Rabi oscillations has not been achieved due to the problems with the AOM. This led to more research about the AOM and how these failures can be prevented in further experiments.

8.1. RABI OSCILLATIONS

When looking at Figure 6.3, no clear Rabi oscillations can be seen. This means that measuring these Rabi oscillations has been unsuccessful. The parameters shown in Table 6.1 give results that are quite likely. However, these parameters are based on the damped oscillation function that has been fitted on our data. And the correlation between these two is only 15.795%, which is too low to draw any conclusions. In Chapter 3, it states that the correlation must be at least 70%, if you want a good measurement.

Thus the Rabi oscillations and the characteristics could not be measured in the end. However, this thesis shows precise timing control of all the signals. In the requirements it states that we must be able to increase the pulse length with steps of $2ns$, which we successfully achieved. Thus it is possible to reuse the scripts again to measure Rabi oscillation in the future. This also means that the scripts that are used to extract different parameters can be reused. This shows that this thesis shows a good basis for further experiments on Rabi oscillations and gate operations.

8.2. AOM

Since the commercially bought AOM broke down during one of the experiments, it was necessary to build a new one. The design that can be seen in Figure 5.12 was created on the crystal. In Chapter 3, it states that this custom-built AOM must be able to react to a signal of $110MHz$, it should be compatible with the old driver and lastly, the efficiency should be more than 96%. These requirements are met, and the AOM still works with the previous driver at a frequency of $110MHz$. The efficiency of the new circuit is 99.986%, which is more than what was required.

However, the AOM was not working when testing it with the driver. This could be due to the crystal, which was damaged too much, or because of the missing piezoelectric material between the copper plates and the crystal.

8.3. OUTLOOK

In the end it was not possible to measure the Rabi oscillations of the system. However, there are multiple scripts that will be sufficient if a new AOM will be available. The custom-built AOM is not working properly and cannot be used due to the damaged crystal. To measure the Rabi oscillations, different devices can be used: a free space AOM, a fiber-coupled AOM or a pulsed laser. Our advice would be to have a pulsed laser or a fiber-coupled AOM. These devices work with a higher accuracy than the free space AOM. The device must be able to turn the laser on and off with a frequency of $1MHz$. This is needed to perform the Rabi oscillations measurements that have been prepared. When one of these devices is available in the lab, the Rabi oscillations can be measured. This also means that the amplitude, Rabi frequency, the phase difference and decay time of the diamond sample can be determined by fitting the data onto 6.1. The Rabi oscillations and the extracting of these quantities can be done with the code that can be found in Appendix A.

BIBLIOGRAPHY

[1] B. Naydenov, F. Dolde, L. T. Hall, *et al.*, "Dynamical decoupling of a single-electron spin at room temperature," *Phys. Rev. B*, vol. 83, no. 8, p. 081 201, Feb. 2011, Publisher: American Physical Society. DOI: 10.1103/PhysRevB.83.081201. [Online]. Available: https://link.aps.org/doi/10.1103/PhysRevB.83.081201 (visited on 06/08/2025).

[2] R. Katsumi, K. Takada, F. Jelezko, and T. Yatsui, "Recent progress in hybrid diamond photonics for quantum information processing and sensing," en, *Commun Eng*, vol. 4, no. 1, p. 85, May 2025, ISSN: 2731-3395. DOI: 10.1038/s44172-025-00398-2. [Online]. Available: https://www.nature.com/articles/s44172-025-00398-2 (visited on 06/08/2025).

[3] D. Aliberti, "MEP_spad_diamond_quantum_biosensing__second_edition_," M.S. thesis, Delft University of Technology.

[4] I. Spoler and K. Vermaat, "Modeling, Simulation, and Validation of Single Photon Avalanche Diodes for NV Center-Based Quantum Sensing," en, 2025.

[5] S. Hernández-Gómez and N. Fabbri, "Quantum Control for Nanoscale Spectroscopy With Diamond Nitrogen-Vacancy Centers: A Short Review," en, *Front. Phys.*, vol. 8, p. 610 868, Feb. 2021, arXiv:2102.06373 [quant-ph], ISSN: 2296-424X. DOI: 10.3389/fphy.2020.610868. [Online]. Available: http://arxiv.org/abs/2102.06373 (visited on 06/08/2025).

[6] J. L. Sánchez Toural, J. García-Pérez, R. Bernardo-Gavito, *et al.*, "Diamond-defect engineering of NV- centers using ion beam irradiation," *Diamond and Related Materials*, vol. 151, p. 111 838, Jan. 2025, ISSN: 0925-9635. DOI: 10.1016/j.diamond.2024.111838. [Online]. Available: https://www.sciencedirect.com/science/article/pii/S0925963524010513 (visited on 04/30/2025).

[7] D. F. S. David J. Griffiths, "Introduction to Quantum Mechanics," English, in *Introduction to Quantum Mechanics*, 3rd ed., University Printing House, Cambridge CB2 8BS, United Kingdom: Cambridge University Press, 2013, p. 527, ISBN: 978-1-107-18963-8.

[8] Wikipedia, the free encyclopedia, *Bloch sphere*, [Online; accessed October 27, 2024], 2024. [Online]. Available: https://en.wikipedia.org/wiki/Bloch_sphere#/media/File:Bloch_sphere.svg.

[9] E. Levine, M. Turner, P. Kehayias, *et al.*, *Principles and techniques of the quantum diamond microscope*, Sep. 2019. DOI: 10.48550/arXiv.1910.00061.

[10] "Fundamentals of magnetic field measurement with NV centers in diamond," English, *Qnami*,

[11] S. V. Titkov, V. V. Yakovleva, I. D. Breev, R. A. Babunts, P. G. Baranov, and N. S. Bortnikov, "NV- center in natural diamonds: Optically detected magnetic resonance study," *Diamond and Related Materials*, vol. 136, p. 109 938, Jun. 2023, ISSN: 0925-9635. DOI: 10.1016/j.diamond.2023.109938. [Online]. Available: https://www.sciencedirect.com/science/article/pii/S0925963523002637 (visited on 04/30/2025).

[12] S. Magaletti, L. Mayer, J.-F. Roch, and T. Debuisschert, "Modelling Rabi oscillations for widefield radiofrequency imaging in nitrogen-vacancy centers in diamond," en, *New J. Phys.*, vol. 26, no. 2, p. 023 020, Feb. 2024, Publisher: IOP Publishing, ISSN: 1367-2630. DOI: 10.1088/1367-2630/ad20b0. [Online]. Available: https://dx.doi.org/10.1088/1367-2630/ad20b0 (visited on 04/30/2025).

[13] Z. Song, H. Yuan, P. Fan, *et al.*, "Enhancing fluorescence of diamond NV- centers for quantum sensing: A multi-layer optical antireflection coating," *Diamond and Related Materials*, vol. 141, p. 110 584, Jan. 2024, ISSN: 0925-9635. DOI: 10.1016/j.diamond.2023.110584. [Online]. Available: https://www.sciencedirect.com/science/article/pii/S0925963523009093 (visited on 04/30/2025).

[14] E. R. MacQuarrie, T. A. Gosavi, A. M. Moehle, N. R. Jungwirth, S. A. Bhave, and G. D. Fuchs, "Coherent control of a nitrogen-vacancy center spin ensemble with a diamond mechanical resonator," EN, *Optica, OPTICA*, vol. 2, no. 3, pp. 233–238, Mar. 2015, Publisher: Optica Publishing Group, ISSN: 2334-2536. DOI: 10.1364/OPTICA.2.000233. [Online]. Available: https://opg.optica.org/optica/abstract.cfm?uri=optica-2-3-233 (visited on 05/02/2025).

[15] V. K. Sewani, H. H. Vallabhapurapu, Y. Yang, *et al.*, "Coherent control of NV- centers in diamond in a quantum teaching lab," *American Journal of Physics*, vol. 88, no. 12, pp. 1156–1169, Dec. 2020, ISSN: 0002-9505. DOI: 10.1119/10.0001905. [Online]. Available: https://doi.org/10.1119/10.0001905 (visited on 05/03/2025).

[16] P. Yu, R. Zhang, R. Zheng, *et al.*, "Coherent manipulation of nitrogen-vacancy centers in diamond via frequency multiplication," *AIP Advances*, vol. 13, no. 6, p. 065 014, Jun. 2023, ISSN: 2158-3226. DOI: 10.1063/5.0147534. [Online]. Available: https://doi.org/10.1063/5.0147534 (visited on 05/03/2025).

[17] D. A. Golter, T. Oo, M. Amezcua, K. A. Stewart, and H. Wang, "Optomechanical Quantum Control of a Nitrogen Vacancy Center in Diamond," *Phys. Rev. Lett.*, vol. 116, no. 14, p. 143 602, Apr. 2016, arXiv:1603.03804 [quant-ph], ISSN: 0031-9007, 1079-7114. DOI: 10.1103/PhysRevLett.116.143602. [Online]. Available: http://arxiv.org/abs/1603.03804 (visited on 05/08/2025).

[18] D. A. Golter, T. Oo, M. Amezcua, I. Lekavicius, K. A. Stewart, and H. Wang, "Coupling a Surface Acoustic Wave to an Electron Spin in Diamond via a Dark State," en, *Phys. Rev. X*, vol. 6, no. 4, p. 041 060, Dec. 2016, ISSN: 2160-3308. DOI: 10.1103/PhysRevX.6.041060. [Online]. Available: https://link.aps.org/doi/10.1103/PhysRevX.6.041060 (visited on 06/08/2025).

[19] R. G. Hunsperger, *Integrated Optics: Theory and Technology*, 6th. New York: Springer, 2009, ISBN: 978-0-387-93898-0. DOI: 10.1007/b98730. [Online]. Available: https://link.springer.com/book/10.1007/b98730.

[20] D. J. McCarron, "A Guide to Acousto-Optic Modulators," en,

[21] University of Arizona, College of Optical Sciences, *Mode-locking hene laser lab manual*, Available online, 2016. [Online]. Available: https://wp.optics.arizona.edu/opti5111/wp-content/uploads/sites/36/2016/04/modelocking_HeNe_Fall2016.pdf (visited on 06/08/2025).

[22] RP Photonics Consulting GmbH, *Acousto-optic modulators*, Online encyclopedia entry, 2024. [Online]. Available: https://www.rp-photonics.com/acousto_optic_modulators.html (visited on 06/08/2025).

[23] Swabian Instruments, *Time tagger x*, https://www.swabianinstruments.com/time-tagger/, 2025.

[24] Zurich Instruments, *Shfsg signal generator*, https://www.zhinst.com/europe/en/products/shfsg-signal-generator, Accessed: 2025-06-16, 2025.

[25] *SHFSG+ User Manual*. [Online]. Available: https://docs.zhinst.com/shfsg_user_manual/index.html (visited on 06/14/2025).

[26] *Welcome to Time Tagger's user manual! — Time Tagger User Manual 2.18.2.0 documentation*. [Online]. Available: https://www.swabianinstruments.com/static/documentation/TimeTagger/index.html (visited on 06/14/2025).

[27] *Zurich Instruments Toolkit 0.7.1 Documentation — zhinst-toolkit documentation*. [Online]. Available: https://docs.zhinst.com/zhinst-toolkit/en/latest/index.html (visited on 06/14/2025).

[28] V. K. Sewani, H. H. Vallabhapurapu, Y. Yang, *et al.*, "Coherent control of nv- centers in diamond in a quantum teaching lab," *American Journal of Physics*, vol. 88, no. 12, pp. 1156–1169, Dec. 2020, ISSN: 0002-9505. DOI: 10.1119/10.0001905. eprint: https://pubs.aip.org/aapt/ajp/article-pdf/88/12/1156/20092348/1156_1_10.0001905.pdf. [Online]. Available: https://doi.org/10.1119/10.0001905.

[29] Isomet Corporation, *Model M1205-T110L-1 Acousto-Optic Modulator Datasheet*, https://isomet.com/PDFacousto-optics_modulators/datasheets-moduvblue/M1205-T110L-1.pdf, Accessed: 2025-05-21, 2023.

[30] Isomet Corporation, *Model 523F-2 RF Driver Datasheet*, https://isomet.com/PDFRFDatasheets/datasheets_ffdrive/553F2+F4+F6.pdf, Accessed: 2025-05-21, 2023.

[31] G. Boivin, P. Belanger, and R. J. Zednik, "Characterization of pure face-shear strain in piezoelectric alpha-tellurium dioxide (alpha-teo2)," *Crystals*, vol. 10, no. 10, 2020, ISSN: 2073-4352. DOI: 10.3390/cryst10100939. [Online]. Available: https://www.mdpi.com/2073-4352/10/10/939.

[32] *VNA Lite User Manual*, Accessed: 2025-06-11, Mini-Circuits, 2023. [Online]. Available: https://www.minicircuits.com/pdfs/VNA_Lite_User_Manual.pdf.

8

[33] Impedans, *The l-shaped matching network*. [Online]. Available: https://www.impedans.com/the-l-shaped-matching-network/.

[34] *RF Inductance Calculator for Single-Layer Helical Round-Wire Coils*. [Online]. Available: https://hamwaves.com/inductance/en/index.html (visited on 06/14/2025).

[35] S. Magaletti, L. Mayer, J.-F. Roch, and T. Debuisschert, *Modelling Rabi oscillations for widefield radiofrequency imaging in nitrogen-vacancy centers in diamond*, arXiv:2309.06203 [quant-ph], Sep. 2023. DOI: 10.48550/arXiv.2309.06203. [Online]. Available: http://arxiv.org/abs/2309.06203 (visited on 05/03/2025).

[36] R. Ghassemizadeh, W. Körner, D. F. Urban, and C. Elsässer, "Coherence properties of NV-center ensembles in diamond coupled to an electron-spin bath," *Phys. Rev. B*, vol. 110, no. 20, p. 205 148, Nov. 2024, Publisher: American Physical Society. DOI: 10.1103/PhysRevB.110.205148. [Online]. Available: https://link.aps.org/doi/10.1103/PhysRevB.110.205148 (visited on 05/21/2025).

A

Overview of code

A.1. ESR Measurement

```
import os
from zhinst.toolkit import Session
import TimeTagger
import numpy as np
from datetime import datetime
import matplotlib.pyplot as plt
from rtcs.devices.zurichinstruments.shfsg_rtcs import ShfsgRtcs

# ======= CONSTANTS ===========
START = 2.85e9
END = 2.89e9
STEP = 1e5
REPETITIONS = 10

# ======= SETUP OUTPUT DIRECTORY ===========
save_dir = "/home/dl-lab-pc3/Documents/Nikolaj_Nitzsche/Rabi_bap"
timestamp = datetime.now().strftime("%Y%m%d_%H%M%S")
save_path = os.path.join(save_dir, f"ESR_{timestamp}")
os.makedirs(save_path, exist_ok=True)
print(f"Saving data to: {save_path}")

# ======= SETUP TIME TAGGER ===========
tagger = TimeTagger.createTimeTaggerNetwork('localhost:41101')
countrate = TimeTagger.Countrate(tagger=tagger, channels=[1])

# ======= SETUP Zurich SHFSG-RTCS ===========
sh = ShfsgRtcs(serial_number='DEV12120')
sh.open()
sh.set_marker_state(0, 1)

DEVICE_ID = 'DEV12120'
SERVER_HOST = 'localhost'
session = Session(SERVER_HOST)
device = session.connect_device(DEVICE_ID)
```

A

```
channel_1 = device.sgchannels[0]

# ======= CONFIGURE CHANNEL 1 ===========
center_frequency = 2.8e9  # 2.8 GHz
synth_1 = channel_1.synthesizer()
device.synthesizers[synth_1].centerfreq(center_frequency)
channel_1.output.on(1)
channel_1.output.range(0)
channel_1.output.rflfpath(1)
channel_1.sines[0].i.enable(1)
channel_1.sines[0].q.enable(1)
awg_1 = channel_1.awg
awg_1.outputamplitude(1)
awg_1.modulation.enable(0)

# ======= SWEEP PARAMETERS ===========
RF_frequencies = np.arange(START, END, STEP)  # 2.85 âĘŠ 2.89 GHz in
                                              100 kHz steps
PL_values = np.zeros((REPETITIONS, len(RF_frequencies)))

# ======= ACQUIRE PHOTOLUMINESCENCE ===========
for rep in range(REPETITIONS):
    for idx, RF_freq in enumerate(RF_frequencies):
        channel_1.oscs[0].freq(RF_freq - center_frequency)
        countrate.startFor(2e11)
        countrate.waitUntilFinished()
        pl_rate = countrate.getData()[0]
        print(f"[Rep {rep+1}/{REPETITIONS}] {RF_freq / 1e9:.6f} GHz âĘŠ
                                              {pl_rate:.0f} counts/s")
        PL_values[rep, idx] = pl_rate

# ======= AVERAGE PL VALUES ===========
avg_pl = PL_values.mean(axis=0)

# ======= NORMALIZE PL (divide by max) ===========
normalized_PL = avg_pl / np.max(avg_pl)

# ======= SAVE DATA ===========
# Raw repeats
np.save(os.path.join(save_path, "PL_values_ESR.npy"), PL_values)
np.savetxt(
    os.path.join(save_path, "PL_values_ESR.csv"),
    PL_values,
    delimiter=",",
    header=",".join(f"{f/1e9:.6f}GHz" for f in RF_frequencies),
    comments=''
)

# ======= AVERAGED===========
np.savetxt(
    os.path.join(save_path, "averaged_PL_ESR.csv"),
    np.column_stack((RF_frequencies, avg_pl)),
    delimiter=",",
    header="Frequency (Hz),PL (counts)",
    comments=''
)
```

A

```
# ======= PLOT: Raw Average PL vs. Frequency ===========
plt.figure(figsize=(8,6))
plt.plot(RF_frequencies/1e9, avg_pl,
         'o-', label="Average PL")
plt.xlabel("Microwave Frequency (GHz)")
plt.ylabel("PL (counts/s)")
plt.title("Average PL vs. Microwave Frequency")
plt.grid(True)
plt.legend()
plt.savefig(os.path.join(save_path, "Average_PL_vs_Frequency.png"),
            dpi=300, bbox_inches='tight')
plt.show()

# ======= PLOT: Normalized PL vs. Frequency ===========
plt.figure(figsize=(8,6))
plt.plot(RF_frequencies/1e9, normalized_PL,
         's-', color='tab:orange', label="Normalized PL")
plt.xlabel("Microwave Frequency (GHz)")
plt.ylabel("PL (normalized)")
plt.title("Normalized PL vs. Microwave Frequency")
plt.grid(True)
plt.legend()
plt.savefig(os.path.join(save_path, "Normalized_PL_vs_Frequency.png"),
            dpi=300, bbox_inches='tight')
plt.show()

print(f"All data and plots saved in: {save_path}")

# ======= CLEANUP ===========
del tagger
sh.close()
session.disconnect_device(DEVICE_ID)
```

A.2. Rabi Oscillation Measurement

```
import os
from zhinst.toolkit import Session
import TimeTagger
import numpy as np
from datetime import datetime
import time
import matplotlib.pyplot as plt


# This function returns 2 items in a list the second item will be the
                                    one for the second trigger and the
                                    first one for the AOM and RF
                                    circuit
def create_seqc_code(pulse_length):
    return [r"""
        wave padding = zeros(2000);
        wave microwave = ones(""" + str(pulse_length * 2e9) + r""");
        wave read_out = zeros(10000);

        setTrigger(0);
```

```
        playWave(1, padding);
        waitWave();
        playWave(1, microwave);
        waitWave();
        playWave(1, padding);
        waitWave();
        setTrigger(1);
        playWave(1, read_out);
        """, r"""
        wave read_out_delay = zeros(""" + str((2e-6 + pulse_length) *
                                              2e9) + r""");
        wave read_out_marker = zeros(10000);

        playWave(1, read_out_delay);
        waitWave();
        setTrigger(1);
        playWave(1, read_out_marker);
        waitWave();
        setTrigger(0);
        """]

# setup output directory
save_dir = "/home/dl-lab-pc3/Documents/Nikolaj_Nitzsche/Rabi_bap"
timestamp = datetime.now().strftime("%Y%m%d_%H%M%S")  # Timestamped
                                                      folder
save_path = os.path.join(save_dir, f"Rabi_{timestamp}")
os.makedirs(save_path, exist_ok=True)  # Create folder if it doesn't
                                       exist
print(f"Saving data to: {save_path}")

# shfsg setup

DEVICE_ID = 'DEV12120'
SERVER_HOST = 'localhost'

# connect to data server
session = Session(SERVER_HOST)

# connect to device
device = session.connect_device(DEVICE_ID)

channel_1 = device.sgchannels[0] # The first channel
channel_2 = device.sgchannels[1] # The second channel

# setup channel 1
synth_1 = channel_1.synthesizer()
device.synthesizers[synth_1].centerfreq(2.8e9)
channel_1.output.on(1)
channel_1.output.range(0)
channel_1.output.rflfpath(1)
channel_1.sines[0].i.enable(1)
channel_1.sines[0].q.enable(1)
channel_1.oscs[0].freq(0.07e9)
channel_1.synchronization.enable(True)
channel_1.marker.source("awg_trigger0")

awg_1 = channel_1.awg
```

A

```
awg_1.outputamplitude(1)
awg_1.modulation.enable(0)

# setup channel 2
synth_2 = channel_2.synthesizer()
device.synthesizers[synth_2].centerfreq(2.8e9)
channel_2.output.on(1)
channel_2.output.range(0)
channel_2.output.rflfpath(1)
channel_2.synchronization.enable(True)
channel_2.marker.source("awg_trigger0")

awg_2 = channel_2.awg
awg_2.outputamplitude(1)
awg_2.modulation.enable(0)

# time tagger setup
counter_channel = 1
trigger_channel = 2

timetagger = TimeTagger.createTimeTaggerNetwork('localhost:41101')


# Set trigger voltage levels and delays to zero to ensure everything is
                                    set to zero
timetagger.setTriggerLevel(counter_channel, 0.25)
timetagger.setTriggerLevel(trigger_channel, 0.5)
timetagger.setInputDelay(trigger_channel, 0)
timetagger.setInputDelay(counter_channel, 0)


# experiment we will sweep the RF from 0.5 microsecond to 4
                                   microseconds with steps of 0.002
                                   microseconds in total 250
                                   repetitions
repetitions = 250 # We will are planning to do 250 so we can do more if
                                    needed
pulse_lengths = np.arange(0.5e-6,4e-6,0.2e-6)
photon_counts = np.zeros((repetitions, len(pulse_lengths)))

# Do the whole experiment for a total of 250 times and then for every
                                   pulse in the pulse train, look
                                   comment above I changed it to it
                                   what I find logical
for repetition in range(repetitions):

    # Count between the rising and falling edge
    counter = TimeTagger.CountBetweenMarkers(tagger=timetagger,
                                        click_channel=counter_channel,

                                        begin_channel=trigger_channel,
                                        end_channel=-trigger_channel,

                                        n_values=len(pulse_lengths) )

    print("Repetition: ", repetition, " / ", repetitions)
    for i,pulse in enumerate(pulse_lengths):
```

```
        # Create and load the sequencer program for both channels
        seqc = create_seqc_code(pulse)
        awg_1.load_sequencer_program(seqc[0])
        awg_2.load_sequencer_program(seqc[1])

        awg_1.enable_sequencer(single=True)
        awg_2.enable_sequencer(single=True)

        time.sleep(0.2)

    pl_rate = counter.getData()
    print(pl_rate)
    print(counter.getBinWidths())
    photon_counts[repetition] = pl_rate

    time.sleep(1)


total_pl = np.sum(photon_counts, axis=0)
print(total_pl)

# # ======= SAVE DATA ===========
np.savetxt(os.path.join(save_path, "PL_values.csv"), photon_counts,
                                    delimiter=",")  # Save as CSV
np.savetxt(os.path.join(save_path, "averaged_PL.csv"), np.column_stack
                                    ((pulse_lengths, total_pl)),
                                    delimiter=",",
           header="Driving Time (ms), PL (counts)")

# # ======= PLOT & SAVE FIGURE ===========
plt.figure(figsize=(8, 6))
plt.plot(pulse_lengths, total_pl, marker='o', linestyle='-', color='b',
                                     label="Total PL vs. Driving Time")
plt.xlabel('Driving Time (ms)')
plt.ylabel('PL (counts)')
plt.title('Total PL vs. Pulse Time (Rabi Oscillations)')
plt.grid(True)
plt.legend()
plt.savefig(os.path.join(save_path, "Rabi_Oscillations.png"))  # Save
                                    plot as PNG
plt.show()

print(f"Data and plot saved in: {save_path}")
```

A.3. AWG Oscilloscope Graphs

```
import matplotlib.pyplot as plt
import csv
import numpy as np

offset = 72
time_offset = 0.748e-5

channel_1_x = []
channel_1_y = []
```

A

```
channel_2_x = []
channel_2_y = []

with open('./ALL0001/F0001CH1.CSV', 'r') as csvfile:
    plots = list(csv.reader(csvfile, delimiter = ','))

    for row in plots[18+offset:]:
        channel_1_x.append(float(row[3][:1] + row[3][2:])+time_offset)
        channel_1_y.append(float(row[4])+2.7)

with open('./ALL0001/F0001CH2.CSV', 'r') as csvfile:
    plots = list(csv.reader(csvfile, delimiter = ','))

    for row in plots[18+offset:]:
        channel_2_x.append(float(row[3][:1] + row[3][2:])+time_offset)
        channel_2_y.append(float(row[4])-0.03)



read_channel_1_x = []
read_channel_1_y = []
read_channel_2_x = []
read_channel_2_y = []

with open('./ALL0002/F0002CH1.CSV', 'r') as csvfile:
    plots = list(csv.reader(csvfile, delimiter = ','))

    for row in plots[18:-offset]:
        read_channel_1_x.append(float(row[3][:1] + row[3][2:])+
                                time_offset)
        read_channel_1_y.append(float(row[4])+1.6)


fig, (ax1, ax3) = plt.subplots(2,1)

color = 'mediumseagreen'
ax1.plot(channel_1_x, channel_1_y, color=color, linewidth=0.8)

ax2 = ax1.twinx()

color = 'goldenrod'
ax2.plot(channel_2_x, channel_2_y, color=color, linewidth=0.8)

color = 'steelblue'
ax3.plot(read_channel_1_x, read_channel_1_y, color=color, linewidth=0.8
                                    )

ax1.set_xticks(np.arange(-0.6e-5, 1.7e-5, 0.1e-5))
ax3.set_xticks(np.arange(-0.6e-5, 1.7e-5, 0.1e-5))
ax1.tick_params(axis='x',labelsize=9)
ax2.tick_params(axis='x',labelsize=9)
ax3.tick_params(axis='x',labelsize=9)
ax1.set_xlabel('Time [s]')
ax3.set_xlabel('Time [s]')
ax1.set_ylabel('Channel 1 Marker [V]')
ax2.set_ylabel('Channel 1 Out [V]')
ax3.set_ylabel('Channel 2 Marker [V]')
```

```
fig.tight_layout()
plt.show()
```

A.4. PIEZOELECTRIC EFFECT PLOT

```
    import pandas as pd
import matplotlib.pyplot as plt
import numpy as np

# Reading file
file_path = "data/F0000CH1.CSV"  # Update path if needed
df = pd.read_csv(file_path, skiprows=2, header=None)
df.dropna(axis=1, how='all', inplace=True)

# Third column can be seen as timing and the 4th as data
df_signal = df[[3, 4]].copy()
df_signal.columns = ['Time (s)', 'Voltage (V)']
df_signal.dropna(inplace=True)

df_signal['Time (ms)'] = df_signal['Time (s)'] * 1000  # To miliseconds
df_signal['Voltage (mV)'] = df_signal['Voltage (V)'] * 1000  # To
                                    millivolts

plt.figure(figsize=(14, 6))
plt.plot(df_signal['Time (ms)'], df_signal['Voltage (mV)'], label='
                                    Channel 1 (TeOâĆĆ)', linewidth=1.2,
                                     color='orange')

plt.xticks(fontsize=16)
plt.yticks(fontsize=16)

plt.title('Piezoelectric Signal from TeOâĆĆ Crystal (Channel 1)',
                                    fontsize=25)
plt.xlabel('Time (ms)', fontsize=20)
plt.ylabel('Voltage (mV)', fontsize=20)
plt.grid(True)
plt.legend(prop={'size': 20})
plt.tight_layout()
plt.savefig("data/piezoelectric_signal.png", dpi=800)
plt.show()
```

A.5. IMPEDANCE MATCHING SIMULATION

```
    import numpy as np
import matplotlib.pyplot as plt
from matplotlib.ticker import ScalarFormatter

ZL = 0.51 - 21.83j

Q = np.sqrt((50 / 0.51) - 1)
C = 1 / (2 * np.pi * 110e6 * Q * 0.51)
L = 50 / Q / (2 * np.pi * 110e6)

L_l = 21.83 / (2 * np.pi * 110e6)
```

A

```
print(L_l)

print(Q,C,L)

def calculate_impedance(f):

    w = 2 * np.pi * f


    Z_ll = 1j * w * L_l

    ZL2 = ZL + Z_ll

    Zc = -1j / (w * C)
    Z1 = ZL2 + Zc

    Zl = 1j * w * L
    Zin = 1 / (1 / Z1 + 1 / Zl)
    return Zin

Z0 = 50
Zin = calculate_impedance(110e6)

Gamma = (Zin - Z0) / (Zin + Z0)
VSWR = (1 + abs(Gamma)) / (1 - abs(Gamma))

print(Zin,Gamma,VSWR)

freqs = np.linspace(100e6, 120e6, 500)
Gamma_vals = []
Zin_vals = []

for f_test in freqs:
    Zin = calculate_impedance(f_test)
    Gamma = (Zin - Z0) / (Zin + Z0)
    Zin_vals.append(Zin)
    Gamma_vals.append(abs(Gamma))

plt.plot(freqs / 1e6, 10 * np.log10(Gamma_vals), color='seagreen')
plt.xlabel("Frequency (MHz)")
plt.ylabel("Return Loss (dB)")
plt.grid(True)
plt.tight_layout()
plt.show()


Zin_vals = np.array(Zin_vals)
Z_mag = 10 * np.log10(np.abs(Zin_vals))
Z_phase = np.angle(Zin_vals, deg=True)

fig, ax1 = plt.subplots()
ax2 = ax1.twinx()

lns1 = ax1.semilogx(freqs, Z_mag, color='teal', label = 'Magnitude')
ax1.set_ylabel("Magnitude (dBÎĪ)")
lns2 = ax2.semilogx(freqs, Z_phase, color='firebrick', label='Phase')
ax2.set_ylabel("Phase (degrees)")
```

```
ax1.set_xlabel("Frequency (Hz)")
lns = lns1+lns2
labs = [l.get_label() for l in lns]
ax1.legend(lns, labs, loc=0)
plt.grid(True)
plt.tight_layout()
plt.show()
```

A.6. PROCESSING THE RABI OSCILLATIONS AND FITTING THE DATA

```
    import pandas as pd
import numpy as np
import matplotlib.pyplot as plt
from scipy.optimize import curve_fit
from scipy.stats import pearsonr

data = pd.read_csv("averaged_PL.csv")
data.columns = ['time', 'PL_counts']
data["PL_smooth"] = data["PL_counts"].rolling(window=5, center=True).
                                    mean()


bounds = ([0, 1e-7, 1e5, -2*np.pi], [20, 1e-3, 1e7, 2*np.pi])


clean_data = data.dropna()
time = clean_data["time"].values

signal = clean_data["PL_counts"].values

# Damping function that described the Rabi oscillations found in the
                                    literature
def damping_function(t,a,b,c,d):
    return a*(1-np.e**(-t/b)*np.cos(c*t + d))

initial_guess = [2, 25e-6, 6e6, 0]

data["PL_smooth"] = data["PL_counts"].rolling(window=5, center=True).
                                    mean()
smooth = clean_data["PL_smooth"].values

params, param_cov = curve_fit(damping_function, time, signal, p0=
                                    initial_guess,  bounds=bounds)
print(params)

fit_signal = damping_function(time, *params)

smooth_norm = (smooth - np.mean(smooth)) / np.std(smooth)
signal_norm = (signal - np.mean(signal)) / np.std(signal)
fit_norm = (fit_signal - np.mean(fit_signal)) / np.std(fit_signal)

smooth_coeff,_ = pearsonr(smooth_norm, fit_norm)
corr_coeff, _ = pearsonr(signal_norm, fit_norm)
similarity_percent = corr_coeff * 100
```

A

```
fitted_frequency = params[2]  # in Hz
print(f"Fitted frequency: {fitted_frequency:.2f} Hz")

print("Correlation: ", similarity_percent)
print("Smooth Correlation: ", smooth_coeff * 100)

plt.figure(figsize=(10, 5))
plt.plot(clean_data["time"] *1e6, signal, label='Original Data', alpha=
                                    0.5)
plt.plot(data["time"] *1e6, data["PL_smooth"], label='Smoothed Data',
                                    linewidth=2)
plt.plot(clean_data["time"]*1e6, fit_signal, '--r', label='Damped
                                    Cosine Fit')
plt.xlabel("RF Driving time (Ī s)")
plt.ylabel("PL Counts")
plt.title("Smoothed Data and Fit")
plt.legend()
plt.grid(True)
plt.tight_layout()
plt.show()
```

A.7. VNA AOM measurement graph

```
from scipy.signal import butter, filtfilt
import matplotlib.pyplot as plt
import numpy as np

file = open("./GOOD-MEASURE.s1p", "r")

data_x = []
data_y = []

lines = file.readlines()[2:]
for lin in lines:
    split = list(filter(None, lin.split(" ")))

    data_x.append(int(split[0]))
    gamma = float(split[1]) + 1j * float(split[2].replace("\n",""))
    imp = (1+gamma)/(1-gamma) * 50
    data_y.append(imp)
    if int(split[0]) == 110000000:
        print(imp)
        print(gamma)
        VSWR = (1 + np.abs(gamma)) / (1 - np.abs(gamma))
        print(VSWR)

Zin_vals = np.array(data_y)
Z_mag = 10 * np.log10(np.abs(Zin_vals))
Z_phase = np.angle(Zin_vals, deg=True)



cutoff = 10
b, a = butter(N=4, Wn=cutoff, btype='low', fs=len(data_x))
```

```
filtered_mag = filtfilt(b, a, Z_mag)
filtered_phase = filtfilt(b, a, Z_phase)

fig, ax1 = plt.subplots()
ax2 = ax1.twinx()

lns1_2 = ax1.semilogx(data_x, Z_mag, color='teal', label = 'Magnitude',
                                    linewidth=1, alpha=0.4, linestyle=
                                    'dashed')
lns1 = ax1.semilogx(data_x, filtered_mag, color='teal', label = '
                                    Magnitude')
ax1.set_ylabel("Magnitude (dBΪΪ)")
lns2_2 = ax2.semilogx(data_x, Z_phase, color='firebrick', label = '
                                    Magnitude', linewidth=1, alpha=0.4,
                                    linestyle='dashed')
lns2 = ax2.semilogx(data_x, filtered_phase, color='firebrick', label='
                                    Phase')
ax2.set_ylabel("Phase (degrees)")
ax1.set_xlabel("Frequency (Hz)")
lns = lns1+lns2
labs = [l.get_label() for l in lns]
ax1.legend(lns, labs, loc=0)
plt.grid(True)
plt.tight_layout()
plt.show()
```